Final Report

Analysis of Surface Particulate Matter and Trace Gas Data Generated during the Houston
Operations of DISCOVER-AQ

AQRP Project 14-009

Prepared for:

Elena McDonald-Buller
Texas Air Quality Research Program
The University of Texas at Austin

Prepared by:

Robert Griffin (Principal Investigator)
Rice University

and

Barry Lefer

University of Houston (now at NASA)

September, 2015

QA Requirements: All input data from the mobile laboratory used in the generation of
this report underwent QA/QC procedures during the original project. At that time, all
such data were reviewed by a non-participating external research team member. All
additional input data (from satellites, other mobile laboratory platforms, stationary
monitors, and CMAQ model output) utilized here were reviewed similarly during
execution of this project.

Executive Summary

       The City of Houston, Harris County, and surrounding areas have a long history of air quality issues because of their large population, extensive industrial activity, and sub-tropical climate. These issues predominantly have been manifested through ozone (O_3) mixing ratios that exceed the National Ambient Air Quality Standards (NAAQS) established by the United States Environmental Protection Agency. However, recent measurements indicate that Harris County barely achieves compliance with the NAAQS that have been established for particulate matter (PM), specifically for particles with diameters less than or equal to 2.5 micrometers ($PM_{2.5}$).

       In recent years, the National Aeronautics and Space Administration (NASA) has placed considerable emphasis on the use of satellite remote sensing in the measurement of species such as O_3 and PM that constitute air pollution. However, additional data are needed to aid in the development of methods to distinguish between low-level and high-level concentrations in these column measurements. To that end, NASA established a program titled Deriving Information on Surface Conditions from Column and Vertically Resolved Observations Relevant to Air Quality (DISCOVER-AQ). DISCOVER-AQ began in summer 2011 with work in the Mid-Atlantic Coast region that featured satellite, airborne, and ground-based sampling; similar work was performed in California in 2012. The DISCOVER-AQ program conducted operations in and near Houston in September 2013 and in and near Denver in 2014.

       During the Houston operations of DISCOVER-AQ, there was a need for ground-based measurement support. A previous project supported by this program filled that need by providing quantitative measurements of sub-micron particle size and composition and mixing ratios of photochemically relevant gases such as O_3 and oxides of nitrogen (NO_x). The instrumentation for these measurements was deployed using the University of Houston/Rice University mobile air quality laboratory. Data quality assurance/control and preliminary data analyses were performed as part of the original project.

       More advanced data analyses have been performed as part of the current project, and results from these analyses are included in this report. These analyses focused on source-specific quantification of PM emissions in a size- and chemically resolved manner, identification of large but short-lived PM events, assessment of the diurnal and spatial distribution of PM in Houston, estimation of the relative oxidation state of organic PM, investigation of the secondary processes that influence PM in Houston, determination of the roles that biogenic volatile organic compounds play in Houston air quality, comparison of *in situ* surface and column airplane and satellite nitrogen dioxide measurement techniques, and photochemical zero-dimensional modeling of O_3 and radical production.

       Key findings of this project include the following:

- Motor vehicular emissions distributed between light-duty, heavy-duty, and gasoline vehicles cause enhancements in organic PM of up to 70 $\mu g\ m^{-3}$ based on emission factors that range from 0.14 to 13.74 grams per mile driven. This PM tends to be relatively chemically reduced;
- Biomass burning events lead to enhancements of organic PM up to 100 $\mu g\ m^{-3}$;

this material also is relatively chemically reduced;
- Petrochemical facilities, in contrast (at least those sampled here) lead to increases in sulfate aerosol;
- The amplitudes and exact timing of PM constituent diurnal profiles vary by location. Nitrate increases at night, sulfate and ammonium co-vary, and organic PM increases significantly during rush hour and only moderately in the afternoon;
- When averaged spatially across the sampling domain, the relative importance (on a mass basis) of specific PM constituents decreases in the following order: organic PM, sulfate, ammonium, nitrate, and chloride.
- With respect to extent of oxidation, organic PM upwind of the city tends to be the most relatively oxidized and that near downtown the least. Downwind oxidation levels are intermediate between the two extremes despite having the highest apparent levels of secondary organic aerosol.
- Sulfate aerosol appears to be driven by regional, as opposed to local, processes, with ammonium concentrations appearing to be driven by those of sulfate;
- Local organic PM processes appear to be governed by nitrate radical oxidation of monoterpenes without the need for liquid water to take up products;
- Isoprene chemistry impacts significantly O_3 formation, which is driven by nitric oxide reactions with (in order) hydroperoxy radicals, non-methyl organic peroxy radicals, and methyl organic peroxy radicals; O_3 termination is driven by the formation of nitric acid; and
- The quality of nitrogen dioxide column and *in situ* measurement comparisons varies depending on selection of spatial resolution and vertical mixing parameters.

Table of Contents

List of Tables

List of Figures

Introduction

The City of Houston, Harris County, and surrounding areas have a long history of air quality issues because of their large population, extensive industrial activity, and sub-tropical climate. These issues predominantly have been manifested through ozone (O_3) mixing ratios that exceed the National Ambient Air Quality Standards (NAAQS) established by the United States Environmental Protection Agency (EPA), as has been documented on the website of the Texas Commission on Environmental Quality (TCEQ). However, recent measurements, particularly near the Houston Ship Channel (HSC), indicate that Harris County barely achieves compliance with the NAAQS that have been established for particulate matter (PM), specifically for particles with diameters less than or equal to 2.5 micrometers ($PM_{2.5}$). Most of these measurements are made near primary sources along the HSC; therefore, it is important to characterize PM in other parts of the region, especially in areas where secondary chemistry is thought to be important. In addition, it is important to quantify and describe the influence of extraordinary events such as long-range dust or biomass burning (BB) plume transport that impact local measurements of PM and other air quality parameters.

In recent years, the National Aeronautics and Space Administration (NASA) has placed considerable emphasis on the use of satellite remote sensing in the measurement of species such as O_3 and PM that constitute air pollution. However, additional data are needed to aid in the development of methods to distinguish between low- and high-level concentrations in these column measurements. To that end, NASA established a program titled Deriving Information on Surface Conditions from Column and Vertically Resolved Observations Relevant to Air Quality (DISCOVER-AQ). DISCOVER-AQ began in summer 2011 with work in the Mid-Atlantic Coast region that featured satellite, airborne, and ground-based sampling; similar work was conducted in California in 2012. The DISCOVER-AQ program conducted operations in and near Houston in September 2013; DISCOVER-AQ completed operations with a campaign in the Denver area during 2014.

During the Houston operations of DISCOVER-AQ, a heavily instrumented NASA airplane was based at Ellington Field. During the ten operation days for this aircraft, flights were conducted that included periods of constant-elevation traverses between points above which spirals were conducted (that is, take off and reach high altitude, cruise at high altitude, spiral down over a pre-defined location, cruise at low altitude, spiral up over a second pre-defined location, cruise at high altitude, spiral down over a third pre-defined location, etc.). The circuit of the Houston area, which took approximately two and a half to three hours to complete, was made three times during each flight day, weather permitting. For these operations, there was a need for ground-based measurement support. Measurements for the original project funded by this program were made across the area to supplement the continuous ground-based monitoring performed by TCEQ, Harris County, the City of Houston, and other entities. For example, as part of the original project, the chemical composition of water-soluble sub-micron PM was measured at the TCEQ Manvel Croix monitoring site located directly south of downtown Houston.

In addition to the flight and stationary ground-based measurements described above, several mobile platforms were operated at the surface to provide additional boundary conditions for the satellite measurements. These platforms were operated by

NASA, Aerodyne Research, Inc., Princeton University, the University of Houston (UH) and Chalmers University collaboratively, and UH and Rice University (Rice) collaboratively. The operations of the UH/Rice platform were the focus of the original project, and more advanced analyses of the data generated are the focus of the current project.

The UH/Rice mobile air quality laboratory (MAQL) generally operated in two modes, determined primarily by occurrence of NASA flight operations. First, during periods when DISCOVER-AQ flights occurred, the MAQL operated in the northwest sector of the Houston metropolitan area at the request of the NASA primary scientific officer for DISCOVER-AQ; the laboratory conducted mobile operations to the extent possible on flight days. The aim was to characterize pollutant outflow (southerly winds) or background air inflow (northerly winds). The route used avoided major highways so that the measurements were not dominated completely by vehicular emissions; the MAQL typically remained at one of the two route endpoints overnight prior to a flight day. The route began in the Tomball area and headed to the Conroe spiral point (or vice versa) and was repeated during flight operations. Generally, this represented downwind conditions, allowing for characterization of secondary pollutants in the Houston plume. Measurements at the Conroe site also allowed for inter-comparison with measurements made by researchers from the University of Texas at Austin; this was part of the quality assurance/control (QA/QC) for the project. On the whole, on-road samples were collected on the order of a quarter of the time during DISCOVER-AQ. Locations and time stamps associated with samples can be found in the data files archived for the original project.

On non-flight days and during periods without downtimes for calibration, instrument maintenance, or crew rest, operations were determined based on coordination with other mobile facilities, meteorology, and several scientific questions and/or objectives. This required a mix of mobile and stationary operations. Some of these objectives include measurements in the HSC and Texas City areas to investigate primary emissions from refinery and petrochemical operations, co-location at Manvel Croix and Conroe to compare multiple instrument data, co-location with the Princeton mobile laboratory that measured ammonia to investigate ammonia-ammonium equilibrium, co-location with other mobile laboratories for inter-comparison purposes, deployment to Galveston to measure inflow on days characterized by southerly flow, sampling near the Washburn Tunnel to characterize vehicular primary emissions, and deployment at various other primary emission sources not affiliated with the petrochemical industry (e.g., landfill, wastewater treatment facility, etc.).

The current project is focused on more detailed analyses of the data generated during the original DISCOVER-AQ project. The work was divided into several tasks, listed here and referred to elsewhere in this report in numerical order:

1.) Determine PM emission rates by particle size by source;

2.) Characterize short-lived but high in local impact increases in PM loadings;

3.) Assess the diurnal character of PM concentrations across Houston;

4.) Assess the relative contributions of PM constituents across Houston;

5.) Estimate the relative extent of oxidation of organic PM as a function of space and time across Houston;

6.) Investigate secondary processes of import with respect to PM in Houston;

7.) Assess the importance of biogenic activity on O_3 and secondary organic aerosol (SOA) formation;

8.) Compare ground-based stationary *in situ* nitrogen dioxide (NO_2) measurements from monitoring stations with available column NO_2 measurements such as satellite and Pandora retrievals to evaluate inter- and sub-pixel variability;

9.) Evaluate the rate of O_3 creation using a zero-dimensional (also referred to as a box) model spatially, temporally, as a function of meteorological conditions, and as a function of nitrogen oxide (NO_x) levels across Houston; and

10.) Evaluate the relative importance of various radical sources across Houston using the same zero-dimensional model.

In addition, data generated by the MAQL and by the stationary sampling at Manvel Croix were made available to other researchers. This report begins with a summary of the original field campaign followed by a description of results and synopsis for each task. It ends with recommendations for future work, a brief discussion of control implications, and concluding remarks.

Field Campaign

This report specifically focuses on a data analysis project. However, in order to put the data in context and to provide background information, a short overview of the field campaign is provided here.

The TCEQ Manvel Croix continuous monitoring station is located at 4503 Croix Parkway in Manvel, TX. It is a short distance from a two-lane (each way) state highway and is located directly adjacent to a local park with sports fields and a playground. There is relatively little vehicular traffic on Croix Parkway due to its being a dead end. During DISCOVER-AQ, logistical support from TCEQ included power upgrades and installation of a trailer to house temporary equipment. Among this temporary equipment was a Brechtel Manufacturing particle-into-liquid sampler (PILS). In the PILS, the inlet is equipped with a cyclone to limit the size of particles in the sample stream to one micron in diameter. The sampled particles are first exposed to steam at high temperature. When the sample flow is cooled, water condenses onto the particles, making them significantly large enough that they are collected easily on an impaction plate when flow direction is changed rapidly. The plate is washed by clean water; soluble material dissolves in the wash water, which is then collected and injected into vials for off-line analysis using ion chromatography (IC). The temporal resolution used for sample collection was one hour to ensure that IC detection limits for three major species (sulfate, nitrate, and ammonium) would nearly always be exceeded. The PILS is equipped with the 1-μm cyclone for comparability to the Aerodyne high-resolution time-of-flight aerosol mass spectrometer (HR-ToF-AMS) described subsequently. The PILS allows a focus on materials that are not amenable to measurement by the HR-ToF-AMS and provides a basis for one method of calculating the collection efficiency of the HR-ToF-AMS (part of QA/QC). Species

measurable (assuming they exceed detection limit) by the PILS-IC include sulfate, nitrate, nitrite, chloride, ammonium, calcium, potassium, magnesium, and sodium. All HR-ToF-AMS data presented here have been corrected for collection efficiency, in part through use of the PILS data.

The MAQL consists of a fiberglass truck body installed in the bed of a full-size pickup, providing approximately 325 ft^3 of air-conditioned laboratory space with ports for *in situ* sampling and remote sensing. A mast mounted meteorological sensor with a global positioning system (GPS) is attached to the front bumper to collect data while stationary and in motion. The vehicle's crew is comprised of two to four scientists, depending on the mission and truck configuration. In the summer of 2012, UH purchased a Chevrolet 3500 HD crew cab one-ton pickup truck with an 8-foot bed and single axle to be the permanent vehicle for MAQL operations. The fiberglass shell has a 40" x 30" sunroof and instrument racks. After accounting for the weight of the fiberglass shell, four instrument racks, four scientists, and a full fuel tank, the MAQL has a usable payload capacity of 2000 pounds for instruments, pumps, and cylinders. The vehicle has been modified to include an adjustable air bag-cushioned suspension, higher capacity tires, three high-capacity alternators, a battery bank, and four inverters for a total science electrical capacity of 10 kW. By placing the 6.5-foot long shell on an 8-foot bed, an additional 30 ft^3 of protected outside storage space is available. The meteorological instruments were mounted on the front bumper to ensure that they are in the free air stream. Table 1 provides a brief overview of the measurements made on the MAQL; more detail is provided in the text that follows. All gases were sampled through a common inlet attached to a movable arm that allowed the samples to be taken from approximately two meters above the ground and approximately one and a half meters in front of the bumper while driving and approximately six meters above ground while in stationary mode. This approach minimized the possibility of sampling air that was disturbed by the vehicle itself. Particles were sampled through a similar inlet that included a 2.5-μm cyclone to limit the plugging of the HR-ToF-AMS caused by large particles. While in stationary mode, the laboratory was operated on shore power if possible; if not possible, the laboratory was parked facing into the wind so that exhaust from a supplementary diesel generator was not sampled. The generator was located behind the inlets (on a trailer hitched to the back side of the MAQL) so that generator exhaust was not sampled while the laboratory was in motion or when parked facing into the wind.

Two instruments were used on the MAQL by the Rice team led by primary investigator (PI) Griffin to characterize the chemical composition and size of aerosol particles. Both instruments sampled from the same inlet. The Rice team performed 1-minute and 20-sec-average measurements of size-resolved aerosol chemical composition using an Aerodyne HR-ToF-AMS while the MAQL operated in mobile and stationary sampling-mode, respectively. In this instrument, sub-micron particles are classified by size according to their speed within a vacuum chamber, which allows estimation of their vacuum aerodynamic diameters. Only sub-micron particles are transmitted through the HR-ToF-AMS lens so here PM refers to sub-micron PM mass (PM_1). Non-refractory material is vaporized, ionized by electron impact, and detected using a time-of-flight mass spectrometer. Based on the ionization/fragmentation pattern, which is quantified using the mass-to-charge ratios (m/z) of the detected ion fragments, the HR-ToF-AMS

provides chemical speciation for ammonium, nitrate, chloride, sulfate, and bulk organic matter (OM). The Rice team also deployed a TSI, Inc. Model AE51 mini-aethalometer on the MAQL to measure black carbon (BC) using an optical absorption technique at a resolution of one minute.

Species	Measurement Technique
Non-refractory PM_1	Aerodyne High-Resolution Time-of-Flight Aerosol Mass Spectrometer
BC	TSI Model AE51 mini-aethalometer
CO	AeroLaser (Garmisch-Partenkirchen, Germany) AL-5001 CO monitor (IR Absorption)
SO_2	Thermo Electron Corp. 43C Trace Level SO_2 Analyzer (Pulsed Fluorescence)
NO_x	Thermo Electron Corp. 42C Trace Level NO-NO_2-NO_X Analyzer (Chemiluminescence)
NO_y	Thermo Electron Corp. 42C-Y NO_y Analyzer (Molybdenum Converter)
O_3	Thermo Electron Corp. 49C O_3 Analyzer (Ultraviolet Photometry)

Table 1. Measurement techniques for various species during the DISCOVER-AQ sampling project on the MAQL. Abbreviations used are defined in the text.

The UH team led by PI Lefer focused on measurement of gas-phase and meteorological parameters (temperature, relative humidity, wind speed, wind direction, and actinic flux). *In situ* O_3 measurements were performed with a Thermo Scientific Model 49C O_3 ultraviolet photometric gas analyzer. Nitric oxide (NO), NO_2, and total reactive nitrogen (NO_y) measurements were made with three modified Thermo Scientific Model 42 trace level chemiluminescence NO-NO_2-NO_x analyzers with a blue light converter (BLC) from Air Quality Design for photolytic conversion of NO_2 to NO and a Thermo molybdenum converter heated to 320°C for conversion of NO_y species to NO. The BLC is more specific in that it essentially converts only NO_2 to NO, compared to the standard molybdenum-based NO_2-to-NO converter used in most EPA and TCEQ air monitoring sites that also converts nitric acid (HNO_3) and peroxy acyl nitrate (PAN)-like compounds to NO and as a consequence tends to over estimate NO_2. Ambient levels of carbon monoxide (CO, a combustion tracer) were measured with a Thermo Scientific CO Analyzer (Model 48C-Trace Level Enhance) with a gas correlation wheel cell that detects CO via the absorption of infrared radiation at a wavelength of 4.6 microns. Ambient levels of sulfur dioxide (SO_2, typically used as a marker for coal combustion for power generation) were monitored using the pulsed ultraviolet fluorescence technique employed in the Thermo Scientific Model 43i-TLE instrument, which takes advantage of the characteristic that SO_2 molecules absorb ultraviolet radiation and then fluoresce in the range of 220 to 240 nm. The UH Atmospheric Radiation Laboratory also deployed a Scanning Actinic Flux Spectroradiometer to measure the solar actinic flux in the

wavelength range of 290 to 560 nm. Photolysis frequencies of NO_2 can be calculated from the actinic flux spectra using the most recent Jet Propulsion Laboratory and International Union of Pure and Applied Chemistry recommendations for absorption cross section and quantum yield data. Meteorological measurements were made from the front of the vehicle as discussed above. These instruments were queried serially every ten seconds with DAQFactory data acquisition software. The GPS data were collected with an integrated antenna/receiver mounted on a plate on the roof of the truck over the driver's head. The meteorological data system received data from the anemometer and GPS, allowing the true wind speed and direction to be calculated by subtracting the vehicle motion from the measured wind speed and direction. Unfortunately, this method of determining winds begins to break down somewhat when there are large differences between the vehicle's speed and wind speed (i.e., trying to resolve light winds when traveling at freeway speeds). Vehicle speed was adjusted as needed by sampling objectives.

All input data from the mobile laboratory used in the generation of this report underwent QA/QC procedures during the original project. At that time, all such data were reviewed by a non-participating external research team member. Minor gaps in the data resulted from normal instrument maintenance, operation, and calibration and from crew downtimes that were necessary for safety purposes. In some cases, this provided a nearly continuous dataset between September 1 and 30, 2013. Again to put the data presented here into context, an overview of the QA/QC information for the funded measurements is given in Table 2; only information for those data used in the analyses presented here is included. Notes on data coverage also are included. All additional input data (from satellites, other mobile laboratory platforms, stationary monitors, and three-dimensional model output) utilized here were reviewed similarly during execution of this project.

Measurement	Relevant species/parameter	Frequency (minimum) of calibrations, zeros, and/or blanks	Information on standards used	Notes (precision, lower detection limits, data coverage, etc.)
HR-ToF-AMS	Sub-micron, non-refractory, size-resolved particle composition (sulfate, nitrate, chloride, ammonium, and OM)	Ionization efficiency (IE)/mass concentration calibration (in addition to pre- and post-campaign): once per 2 weeks; Size distribution calibration: once per 2 weeks; inlet flow calibrated once per 2 weeks (or as needed post repair or other event)	IE: Ammonium nitrate obtained from Fisher Scientific (99.8% assay) was used to create a solution that was atomized; particles were size-selected using a differential mobility analyzer. Size: Atomized National Institute of Standards (NIST)- traceable polystyrene latex spheres; Flow calibration performed using a DryCal	Lower detection limit < 200 ng m^{-3} for all species; estimated uncertainty $\pm 25\%$, data coverage during the first half of the month approximately 50% due to electronic issues associated with mobile measurements; essentially 100% after repair outside of planned calibrations, data downloads, and similar activities
PILS	Sub-micron, water-soluble particle ionic species (sulfate, nitrate, nitrite, chloride, ammonium, calcium, sodium, magnesium, and potassium)	ICs calibrated with 6 point standard curves pre- and post-offline analysis; background check once per day for one hour; PILS inlet flow calibrated using mass flow meter at start and end of campaign	Seven anion-II and six cation-II standard mixed solutions obtained from Dionex Corporation	Data missing only during short unplanned instrumental issues/malfunction. Resulting data coverage (outside of calibrations and power failure) near 95% (includes data below detection limit). Approximate lower detection limits: 0.15 µg m^{-3} for all anions and 0.25 µg m^{-3} for all cations

Meteorological	Temperature, relative humidity, wind speed, wind direction, radiation	Calibrated at UH prior to and after deployment or factory calibrated	Calibrations performed at UH with equipment from the manufacturer (RM Young)	Data coverage essentially 100%
UH Trace Gases	O_3, CO, SO_2, NO, NO_2, NO_y	Span/zero checks were performed nightly on all gas instruments, including pre- and post-campaign. Each instrument was given a multi-point challenge several times per week via the sampling inlet. Additionally, NO, NO_y, SO_2, and CO were zeroed roughly every 53 minutes to determine baseline drift. NO_2 was zeroed every 10s as part of the measurement cycle.	Zero air displacement calibrations were created by blending air from an AADCO 737 zero air generator and 2% NIST Scott-Marin CO, SO_2, NO, and NO_2 gases in a TEI 146i. Ozone levels were generated with a TEI 49c-PS traceable to the EPA Region 6 Standard Reference Method. Calibrations were performed at night either in a UH facility or on-site using shore power as calibration equipment was located on a truck separate from the mobile facility.	Data coverage essentially 100% except for during a pump failure on the NO_y instrument. Uncertainties: 4% for O_3, CO, SO_2, NO, and NO_y; 7% for NO_2 Detection limits: 1.5 ppb, 40 ppb, 60 ppt, 30 ppt, 50 ppt, and 110 ppt (for gas order above, respectively)

Table 2. QA/QC overview for the instrumentation on the MAQL during DISCOVER-AQ.

Results and Discussion – Task 1

The focus of Task 1 is the understanding of size-resolved and chemically speciated emissions of PM. Here, only on-road vehicular emissions are considered, and a protocol for determination of emission factors from specific vehicle types (heavy duty, light duty, gasoline, etc.) was derived; relevant particles sizes for all of these emissions were on the order of 1-200 nm in diameter. Other large spikes of PM concentration are considered further in Task 2.

A ratio of measured enhancements in organic aerosol (OA) to enhancements in either CO or NO is compared to known emission factors for CO or NO (taken from the EPA MOtor Vehicle Emission Simulator, MOVES2014). Enhancements (over three standard deviations) are defined relative to the background (termed a delta) immediately before and after the plume sampling. Plumes of OA while the MAQL was on-road were identified for the DISCOVER-AQ period, and the corresponding enhancements in OA, CO, and NO were calculated. Fifteen specific episodes were identified for on-road emissions; enhancements in sub-micron OA ranged from 14 to 71 μg m^{-3}. On-road sources were confirmed through a meticulous review of the video footage, which also allowed for an estimate of the nearby fleet distribution (amount of diesel versus gasoline, amount of light-duty versus heavy-duty, etc.). It should be noted that $\Delta CO:\Delta NO_x$ molar ratio (defined using the colon) values from identified events do not appear to depend on fleet composition (percentage of diesel/heavy-duty vehicles).

The bulk $CO:NO_x$ emission ratios calculated from the EPA MOVES2014 for Houston/Harris County for the month of September 2013 are ~0.58 for diesel vehicles and ~7.75 for gasoline vehicles. However, emission ratios can vary significantly due to changes in driving conditions, temperature, and other factors. For the conversion of measured $OA:NO_x$ or $OA:CO$ ratios to emission factors (EF) of OA (g OA emitted per mile driven), weighted averages of EFs for CO and NO_x were estimated based on fleet composition assuming that all heavy-duty vehicles identified in the videos collected on the MAQL have diesel engines and that all light-duty vehicles and motorcycles are gasoline-based. The EF of OA was then taken as the product of the EF for CO times the observed $OA:CO$ ratio or as the EF for NO_x times the observed $OA:NO_x$ ratio; both formulas were used in order to provide a range of potential values. These vehicle EFs for OA are rough estimates of how much OA is emitted per mile driven for the average fleet composition encountered by the MAQL during the events. These values may not be representative of the OA EFs for the vehicle fleet in Houston/Harris County. Large variability exists between the EF of OA values predicted from CO and NO_x measurements and between different vehicles (in some cases, up to more than an order of magnitude; the range of values obtained is 0.14 to 13.74 g OA per mile driven).

Results and Discussion – Task 2

Task 2 characterizes large PM concentration events that are short in temporal duration (order minutes). Time and location were identified based on GPS data, and the increases in OA or sulfate concentration compared with local background levels were calculated (again, a delta, as defined in Task 1). Based on video observations, the probable source associated with each of the observed events was determined. Twenty-six PM statistically defined (three standard deviations) peak events were observed during the

mobile-mode operation of the mobile laboratory. From these, fifteen, six, and four episodes of high PM concentration were associated with traffic activity (discussed in Task 1), industrial sources (specifically chemical and petrochemical facilities), and BB activities, respectively. The responsible source(s) for one of the observed PM peak events was not identified due to deficient light conditions and the resulting low resolution of the video records. This event was not included in any of the analyses for Task 2 described subsequently.

The average fleet composition during the PM peak events associated with mobile sources was analyzed. Light-duty vehicles were predominant in 50% of the traffic-related events, while heavy-duty vehicles and light-duty trucks were the main component of the fleet in 28.6 and 21.4% of the PM peak events associated with vehicle emissions, respectively. Four of the traffic-related PM peak events were connected with single vehicles from which plumes were identified clearly. Not surprisingly, OA was found to be the main constituent of the submicron PM in the traffic-related peaks, with a range of increase in concentration of 14 to 71 μg m^{-3} compared with local background levels. Examples of peak traffic-related events are shown in Figure 1, which shows time series of PM material concentration enhancements (up to approximately 20 μg m^{-3}) and identifies large peaks by probable vehicle type (in these cases heavy duty) based on video footage.
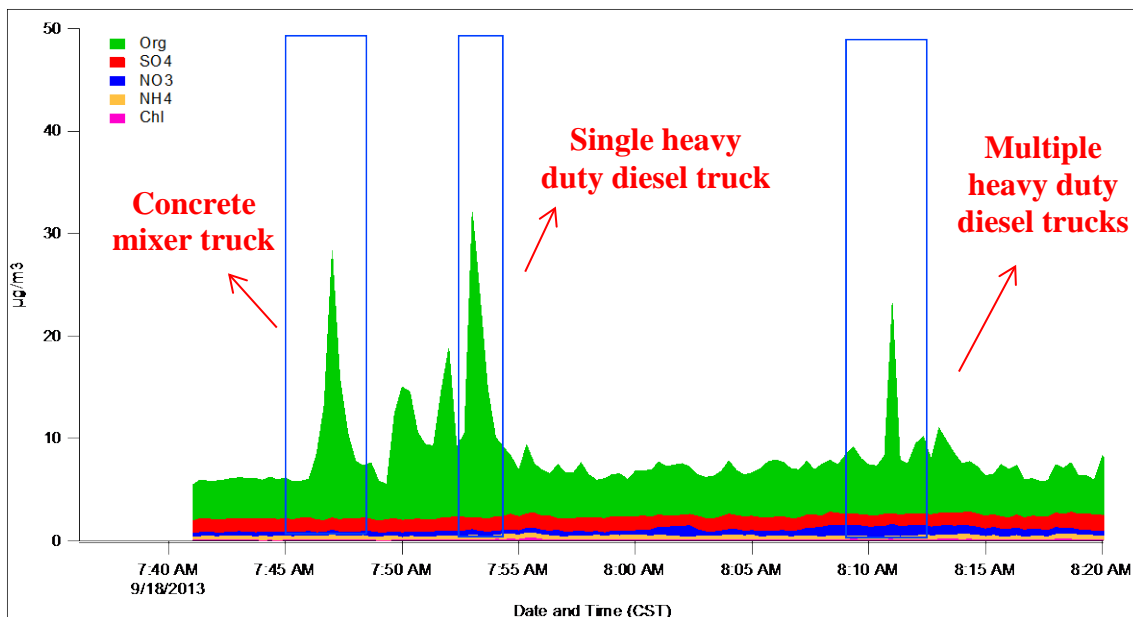
Figure 1. Time series of HR-ToF-AMS concentrations during a peak event associated with traffic.

Sulfate was the largest component of the peak events identified in the perimeter of three industrial complexes, including those associated with petrochemical and refining activities. More moderate increases in the organic and ammonium fraction of PM compared with the specific background concentrations were also noticed in these peaks. Average enhancements in sulfate levels in the identified industrial-related peaks ranged between 3 and 30 μg m^{-3}. An example of a peak industrial facility event is shown in

Figure 2, which shows time series of PM material concentrations and identifies large peaks by probable specific source type (gas flares and storage tanks) based on video footage within the plant area.
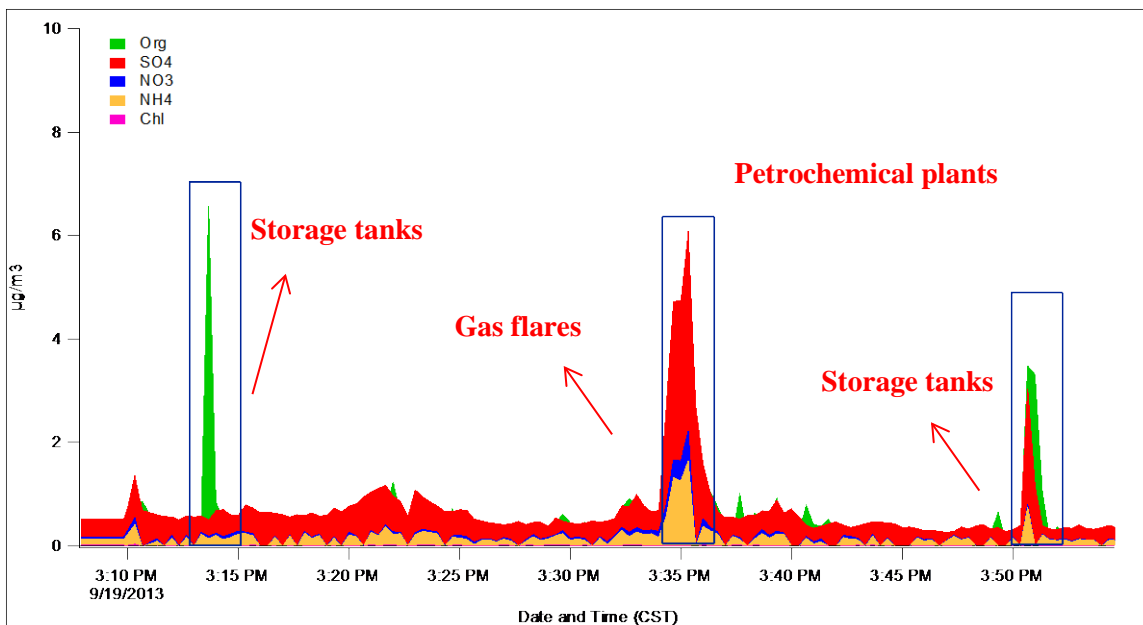
Figure 2. Time series of HR-ToF-AMS concentrations during a peak event associated with industry.

Peak events associated with BB showed high concentrations of OA, indicating significant increases of this component compared with its local background levels. Average enhanced OA concentrations in these peaks varied between 16 and 107 μg m^{-3}. An example of a peak BB event is shown in Figure 3, which shows time series of PM material concentrations.

Although comprehensive bulk characterization of the organic fraction of the measured PM will be conducted by application of positive matrix factorization (PMF) (Task 5), analysis of the character of the OA during peak events was performed based on (i) metrics related to the oxidation state of the constituents of this fraction and (ii) specific mass spectral (MS) tracers for hydrocarbon-like organic aerosols (HOA), which are used as a proxy for primary organic aerosol (POA). The ratios of oxygen to carbon (O:C), hydrogen to carbon (H:C), and organic mass to organic carbon (OM:OC) of the organic fraction of PM are considered (Aiken et al., 2008; Canagaratna et al., 2015).

For traffic activity, the average O:C, H:C, and OM:OC were 0.11 ± 0.04 (one standard deviation), 1.85 ± 0.07, and 1.32 ± 0.08, respectively. The O:C and OM:OC values agree with previously reported ratios for emissions from diesel and gasoline vehicles (O:C between 0.06 and 0.1 and OM:OC ranging between 1.2 and 1.3) (Aiken et al., 2008; Canagaratna et al., 2015). No specific correlation was observed between predominant vehicle type in the fleet and O:C, H:C, and OM:OC ratios. An observed decrease in O:C in the PM peaks when compared with the background levels (average background O:C of 0.38 ± 0.12) indicates a lower oxidation state of the OA emitted by

11

the vehicles, which concurs with the expected predominance of primary HOA in these peaks. This observation is supported by the increase in the H:C value for the selected events (average background H:C of 1.59 ± 0.15). A strong correlation between OM:OC and O:C ($R^2 = 0.994$) suggests very little contribution from nitrogen or other non-oxygen atoms in this POA. Figure 4 illustrates these facts by comparing the values of these metrics during peak traffic events to those representative of the background.
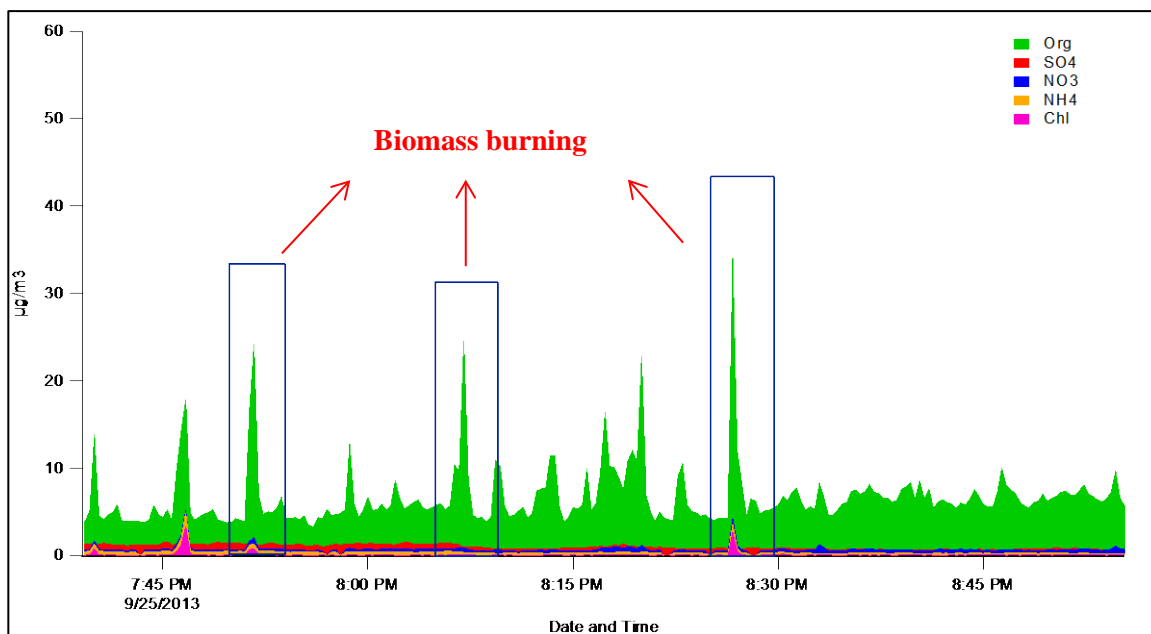
Figure 3. Time series of HR-ToF-AMS concentrations during a peak event associated with burning activity.

The average O:C, H:C, and OM:OC values for the peak events associated with BB are 0.31 ± 0.016, 1.63 ± 0.04, and 1.56 ± 0.022, respectively. As with the traffic-related PM peaks, a decrease in the oxidation state of the OA compared with the background levels was noticed. This observation is consistent with the expected primary character of the aerosol in plumes generated by BB activities. Values for O:C between 0.3 and 0.4 have been reported previously for BB plumes, agreeing with these observations (Aiken et al., 2008; Canagaratna et al., 2015). The primary character of the OA in the BB-related events is confirmed by an increase in the H:C ratios. These metrics are exemplified in Figure 5, which contains the same information as Figure 4, only applied to the BB events.

More moderate differences between O:C in the background and peak event OA are noticed for peaks associated with BB plumes when compared to traffic–related peaks (average reductions of approximately 30 and 70%, respectively). This observation indicates the highly reduced and likely primary character of the OA in the PM peaks from vehicle emissions. The average OM:OC for the PM peaks produced by traffic activity was lower than that observed for the BB events, agreeing with previous research reporting the trend HOA < BB OA < oxygenated OA (OOA) for this ratio (Aiken et al., 2008).
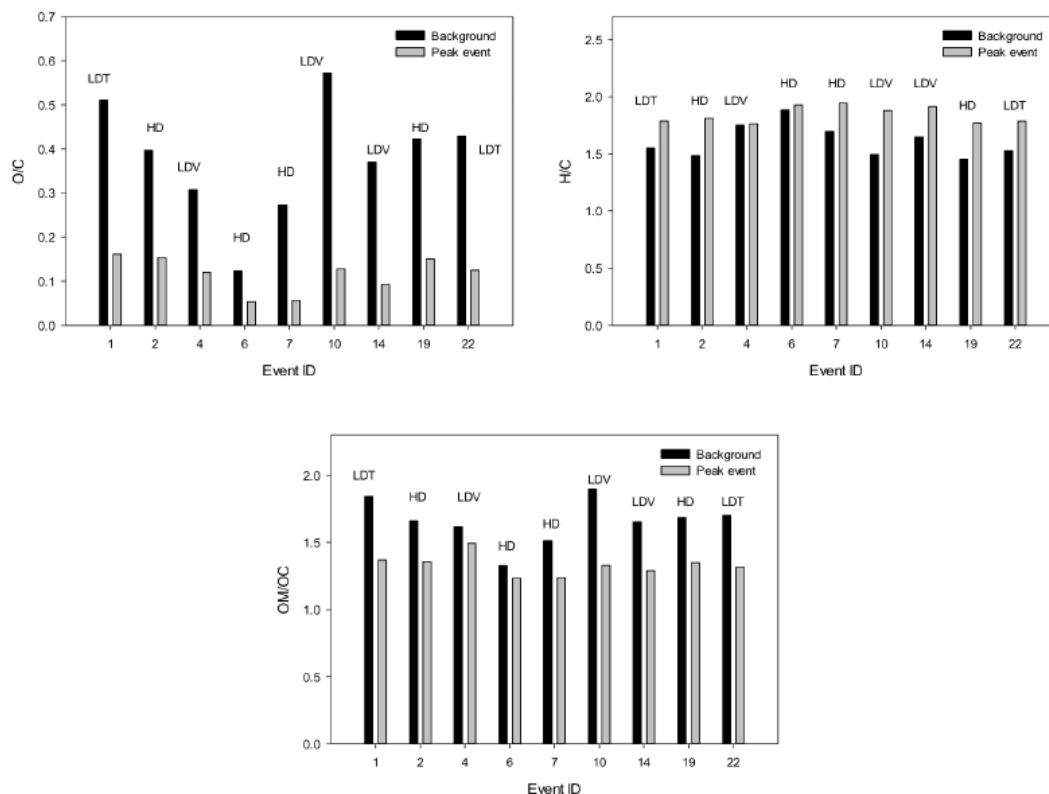
Figure 4. Oxidation metric values and predominant fleet component (LD = low duty, HD = heavy duty, V = passenger vehicle, T = truck) for selected traffic-related peak events. Event ID numbers are the peak event identifier in chronological order.

In addition to the oxidation state of the OA as characterized by these ratios, the enhancement of specific MS fragments associated with combustion emissions in the identified peak events was examined (Canagaratna et al., 2007). The signals at m/z 43, 55, and 57 have been used as tracers for HOA, and it has been demonstrated that they exhibit strong correlation with markers of combustion emissions such as CO and NO_x. As other oxygenated species may impact m/z 43 and 55, and their correlations with CO and NO_x are usually weaker than that for m/z 57, m/z 57 has been considered as a more reliable tracer for HOA. An increase in the m/z 57 signal was observed for the entire set of peak events associated with vehicle emissions, an example of which is shown in Figure 6. The increase relative to background ranged between 0.32 and 2.34 equivalent mass units ($\mu g\ m^{-3}$), with an average of 0.79 ± 0.63. The highest value was observed for an event in which two diesel light duty trucks were identified as the responsible sources of the increase in the PM concentration. These results are consistent with observations obtained from analysis of the O:C, H:C, and OM:OC ratios and confirm the primary character of the OA present in the traffic-related PM peaks observed during the DISCOVER-AQ field campaign.
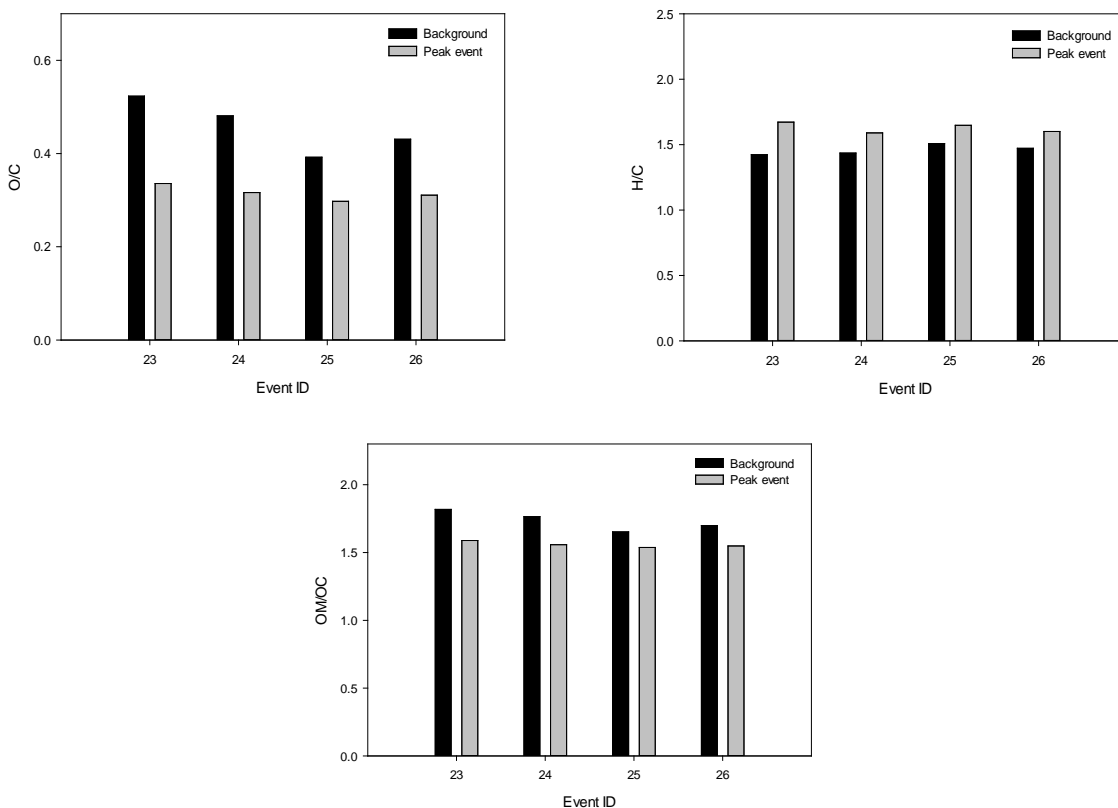
Figure 5. Oxidation metric values for selected BB-related peak events. Event ID numbers are the peak event identifier in chronological order.
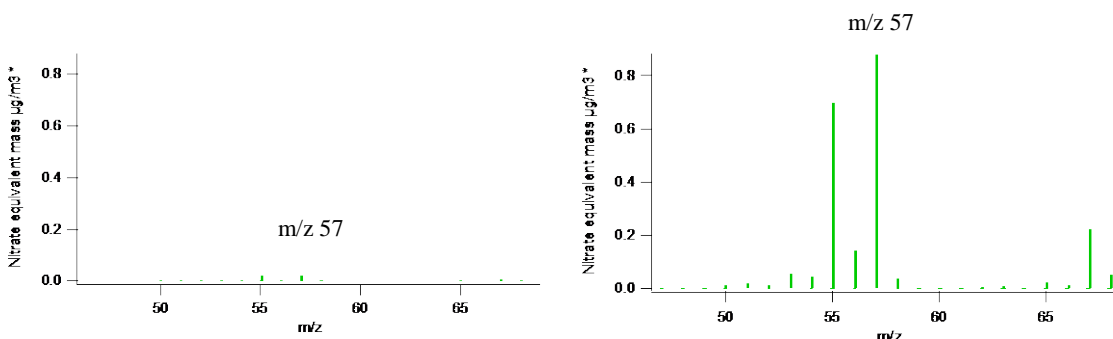
Figure 6. Signal of m/z 57 fragment for a selected peak event associated with traffic activity: background signal (left) and peak event (right).

Results and Discussion – Task 3

The temporal variation of the submicron PM concentration in Houston during the DISCOVER-AQ field campaign was studied in Task 3 using the data obtained during stationary and mobile operations of the MAQL. Stationary operation of the MAQL was conducted mainly at five different field sites: Conroe (co-located with scientists from University of Texas - Austin), Spring Creek Park, Manvel-Croix (co-located with scientists from Baylor University as well as the PILS described previously), San Jacinto,

and Galveston. The length of the MAQL operation at each location varied among sites (typical deployment periods comprised several hours during different days).

The diurnal character of different PM constituents at Conroe, Spring Creek Park, and Manvel Croix during DISCOVER-AQ has been evaluated. The limited size of the PM particle composition datasets collected at the San Jacinto and Galveston locations prevent a statistically meaningful analysis of the diurnal variations of OA, sulfate, ammonium, and nitrate at these sites. The diurnal profiles of four PM species in Conroe, Spring Creek Park, and Manvel Croix are shown in Figure 7, Figure 8, and Figure 9, respectively. In addition to considering the diurnal profile of specific PM constituents, the diurnal profiles of various low-resolution metrics of the extent of oxidation are considered for these same locations. These markers include the average carbon oxidation state (OSc (Kroll et al., 2011), H:C, and O:C. All diurnal profiles depend strongly on location and show considerable variability, likely due to the non-consecutive nature of the datasets that are being used to generate the diurnal profiles from the HR-ToF-AMS. These diurnal profiles are shown in Figure 10.
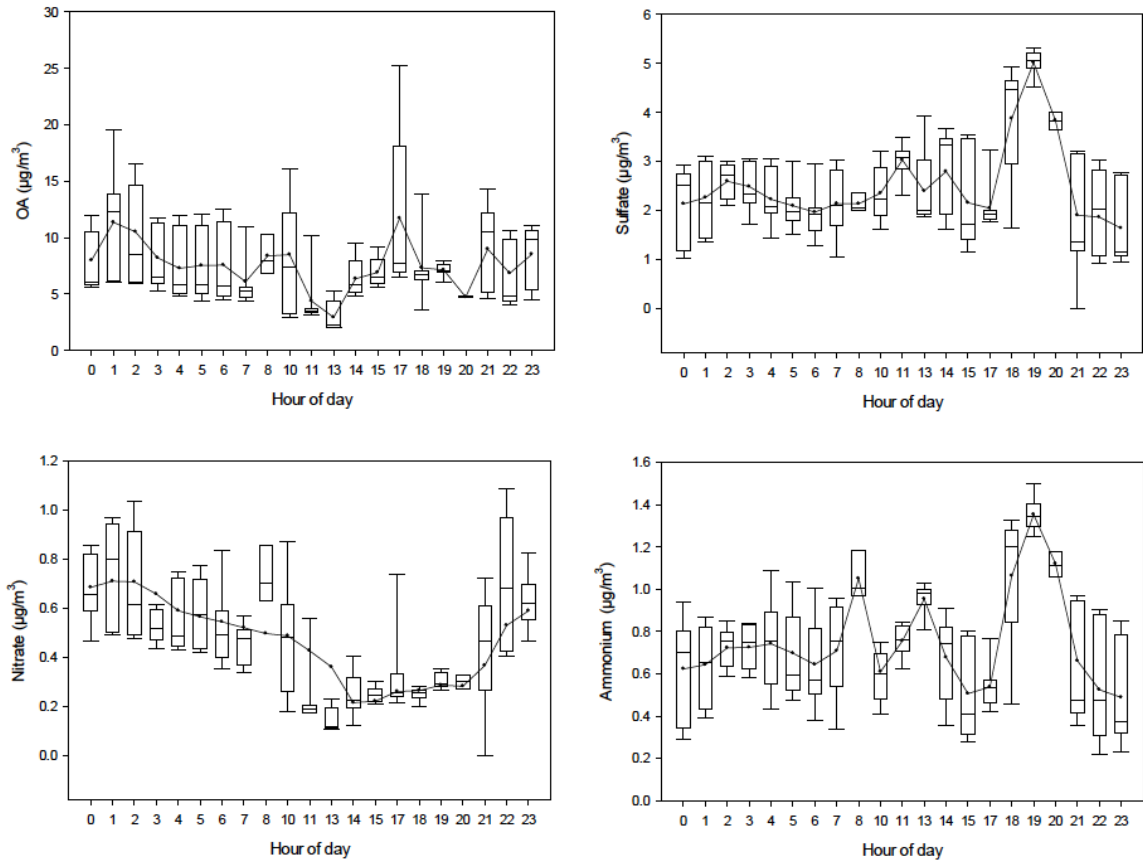
Figure 7. Diurnal pattern of OA (top left), nitrate (bottom left), sulfate (top right) and ammonium (bottom right) at Conroe during DISCOVER-AQ. Dots and line represent means; boxes represent 25th, 50th, and 75th percentiles, and whiskers the 5th and 95th.
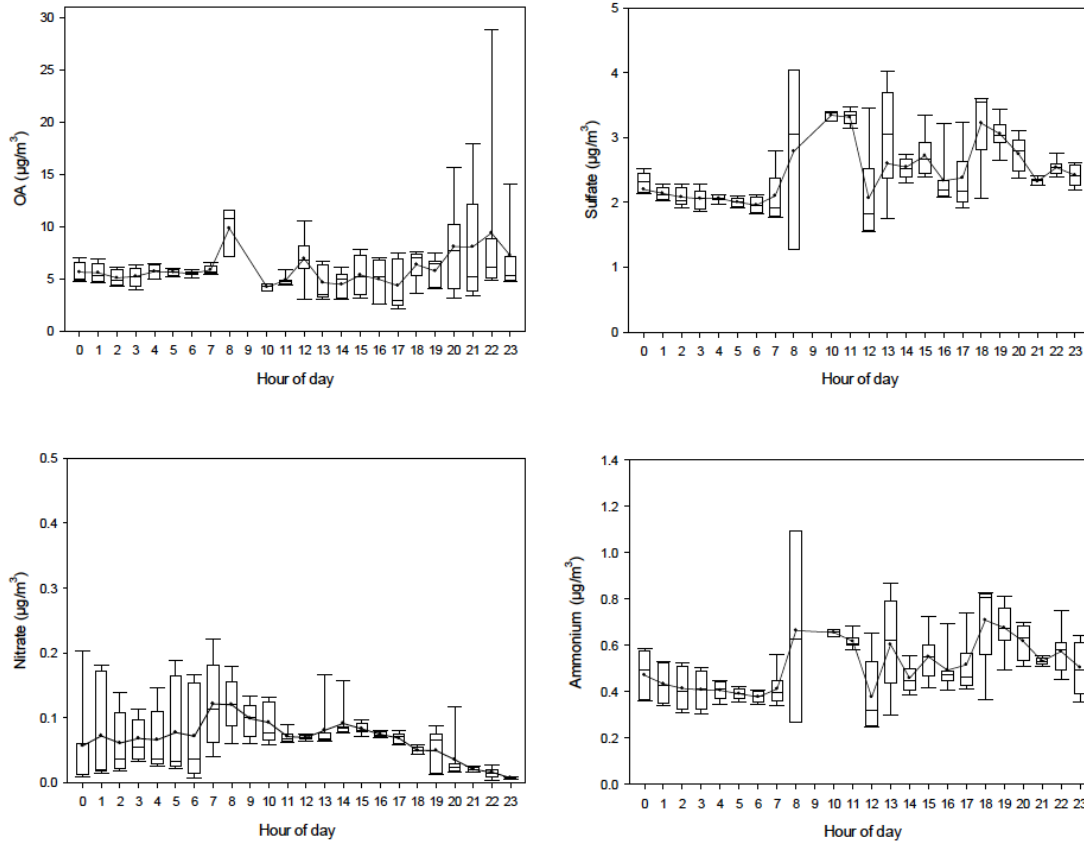
Figure 8. As in Figure 7 but for Spring Creek.
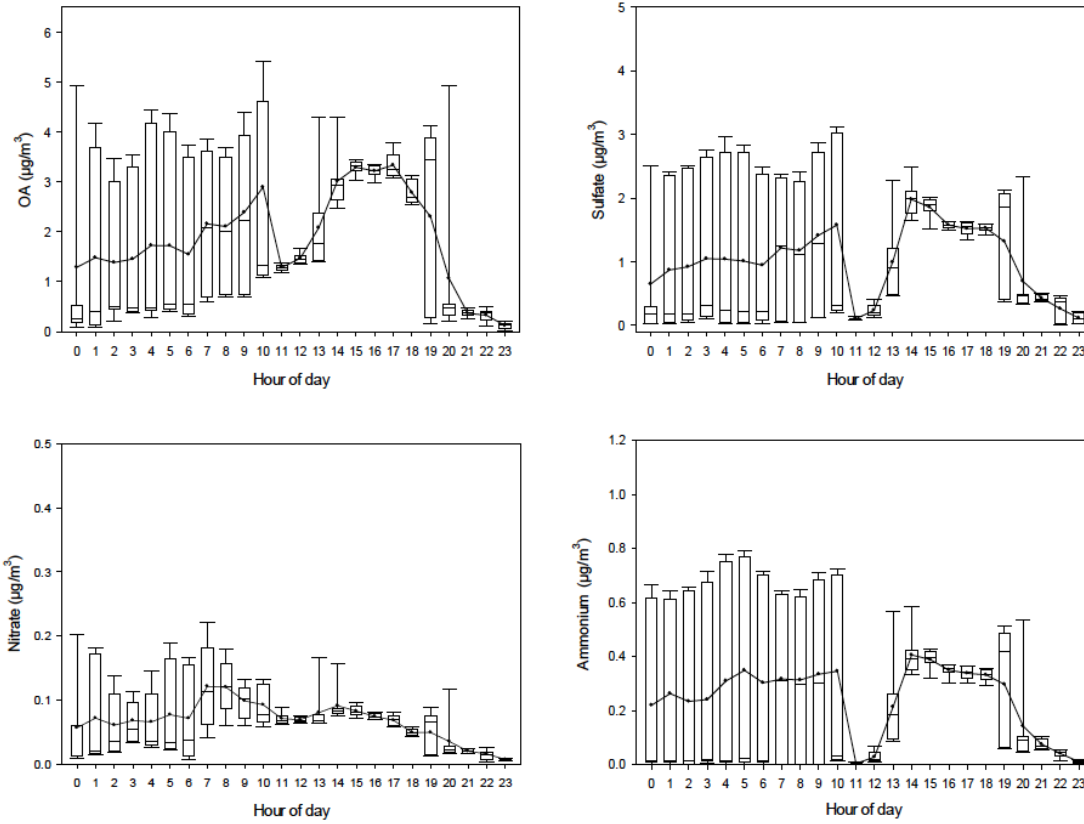
Figure 9. As in Figure 7 but for Manvel Croix.
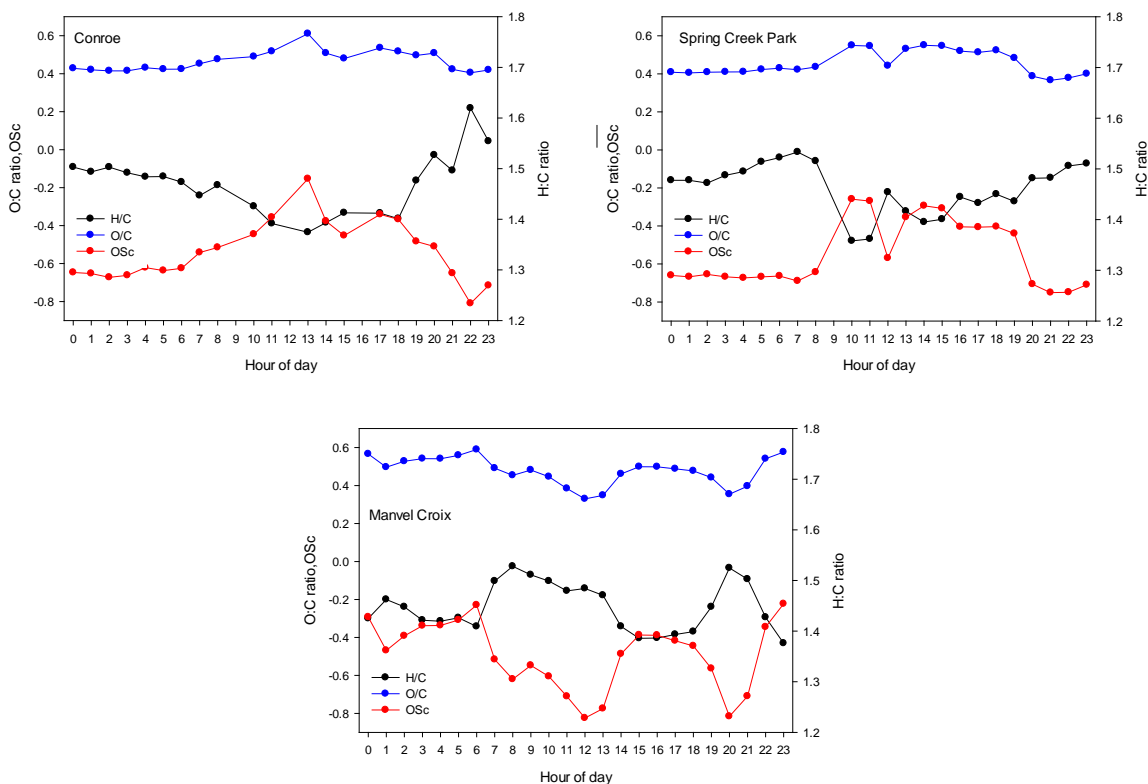
Figure 10. Diurnal pattern of O:C (blue), H:C (black), and OSc (red) for Conroe (top left), Spring Creek (top right), and Manvel Croix (bottom). For simplicity, only means are shown.

Based on consideration of Figure 7, Figure 8, Figure 9, and Figure 10, some general observations include:

- Particulate nitrate concentrations at Conroe and Spring Creek Park exhibit a similar diurnal pattern with a marked decrease of concentration during the day and increasing concentration during the night, as typically observed for this species during summer. Concentrations of this PM constituent at Manvel Croix differ from this pattern, with more moderate daytime decreases and nighttime increases.

- Diurnal profiles of OA concentration show different trends at these three field sites. However, a common moderate peak of concentration is observed at from 8:00 to 10:00 Central Daylight Time (CDT), corresponding with the period of traffic emissions during rush hour. A pronounced broad peak in OA concentrations in the afternoon hours is observed at the Manvel Croix field site, while a more moderate peak is observed at Conroe during the same period of time. This peak is likely associated with formation of SOA as indicated by the corresponding peaks in O:C and OSc, particularly at Manvel Croix. Reductions in H:C and increases in O:C and OSc are observed during daytime (8:00 to 20:00 CDT) at the Conroe and Spring Creek Park locations, indicating the prevalence of SOA during this period. A peak in OSc is observed at approximately 13:00 CDT at the Conroe site, while a double peak

19

earlier in the morning (9:00-10:00 CDT) and between 13:00 and 16:00 CDT is observed for this metric at Spring Creek Park.

- The diurnal profiles of H:C, O:C and OSc at Manvel Croix site exhibit an increase in H:C during the morning hours (6:00-13:00 CDT), indicating the predominance of POA. This increase is followed by a reduction during the afternoon hours (13:00-18:00 CDT) and a corresponding increase in O:C and OSc during this period of time, indicating the formation of SOA.

- Concentrations of particulate sulfate at the Conroe and Spring Creek Park sites exhibit a characteristic peak from 10:00 to 12:00 CDT associated with early emissions of SO_2, potentially related to traffic activity. An atypical peak of sulfate concentration is observed from 18:00 to 20:00 CDT at the three monitoring locations, with more pronounced increases occurring at Conroe. This could be related to the statistics of a relatively small number of data points because sulfur to sulfate conversion usually occurs on longer time scales (Wojcik and Chang, 1997); another hypothesis is the transport of directly emitted sulfate to the sampling sites.

- The diurnal variations of sulfate and ammonium concentrations show a similar pattern within each sampling site, indicating that ammonium is associated predominantly with sulfate in the aerosol.

Results and Discussion – Task 4

The spatial variation of the submicron PM composition across Houston during the DISCOVER-AQ field campaign was studied in Task 4 using the data obtained during stationary and mobile operations of the MAQL. First, the relative contribution of OA, sulfate, nitrate, ammonium, and chloride to PM at the five selected field sites where the MAQL operated in stationary mode was considered. On a mass basis, OA was the predominant species at the Conroe, Spring Creek Park, Manvel Croix and San Jacinto locations, followed by sulfate, ammonium, nitrate, and chloride. The average contribution of OA ranged between 50.7 and 71.9 %, with highest and lowest percentages observed at the Conroe and San Jacinto sites, respectively. Sulfate concentrations constituted between 20.2 and 39.1% of the PM at these four locations, with highest and lowest percentages observed at San Jacinto and Conroe, respectively. Ammonium contribution to PM varied between 4.5 and 8.9%, while nitrate and chloride constituted between 1.1 and 3.2% and between 0.1 and 0.3% of PM, respectively. In contrast, sulfate was the predominant PM species at Galveston (47.8%), followed by OA, ammonium, nitrate, and chloride. Based on mobile sampling across several locations in Houston with varying concentration of PM, OA and sulfate are the predominant constituents of the submicron aerosol. Percentage contributions of OA as high as approximately 81% were detected in locations influenced by high traffic activity in south Houston (Sam Houston Parkway, SHP), while smaller contributions of OA were observed on the west side of Houston near SHP (55-60%). These results are summarized in Figure 11.
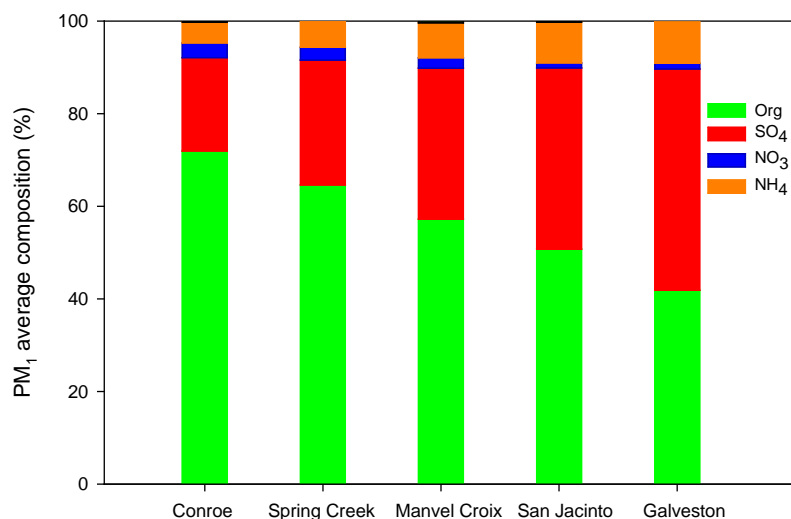
Figure 11. Average contribution of PM constituents at five selected field sites for stationary operation of the MAQL during DISCOVER-AQ.

A more comprehensive analysis of the spatial distribution of PM constituents across Houston was conducted by partitioning the Houston area where the MAQL was located (both mobile and stationary-mode operations) during DISCOVER-AQ into square grids of one square kilometer. Calculation of the average concentrations of PM, OA, sulfate, nitrate, ammonium and chloride, along with the average contribution of OA and sulfate to PM, in each grid was performed. Patterns such as the consistent dominance of OA in PM across Houston, largest contributions of OA and nitrate in downwind areas (in this case to the northwest of downtown Houston), and the presence of locations with percentage contributions of sulfate above 50% (particularly in East Houston, which are tracked by ammonium contributions) can be observed from the spatial segregation of the data.

Further spatial information was garnered through statistically dividing data into geographic zones using a two-step cluster analysis applied on data acquired in stationary-mode operation; this cluster analysis is based not only on physical location but also on OSc values and OA concentrations. These zones are defined roughly as Zone 1 (northwest), Zone 2 (central), and Zone 3 (east/southeast). Values are summarized in Figure 12 and Table 3. The total concentrations are largest (by a factor of approximately two) in the downwind Zone 1. While not exact, wind direction was relatively consistent for the time periods described by Figure 12, indicating that differences are unlikely to be related to variations in meteorology.
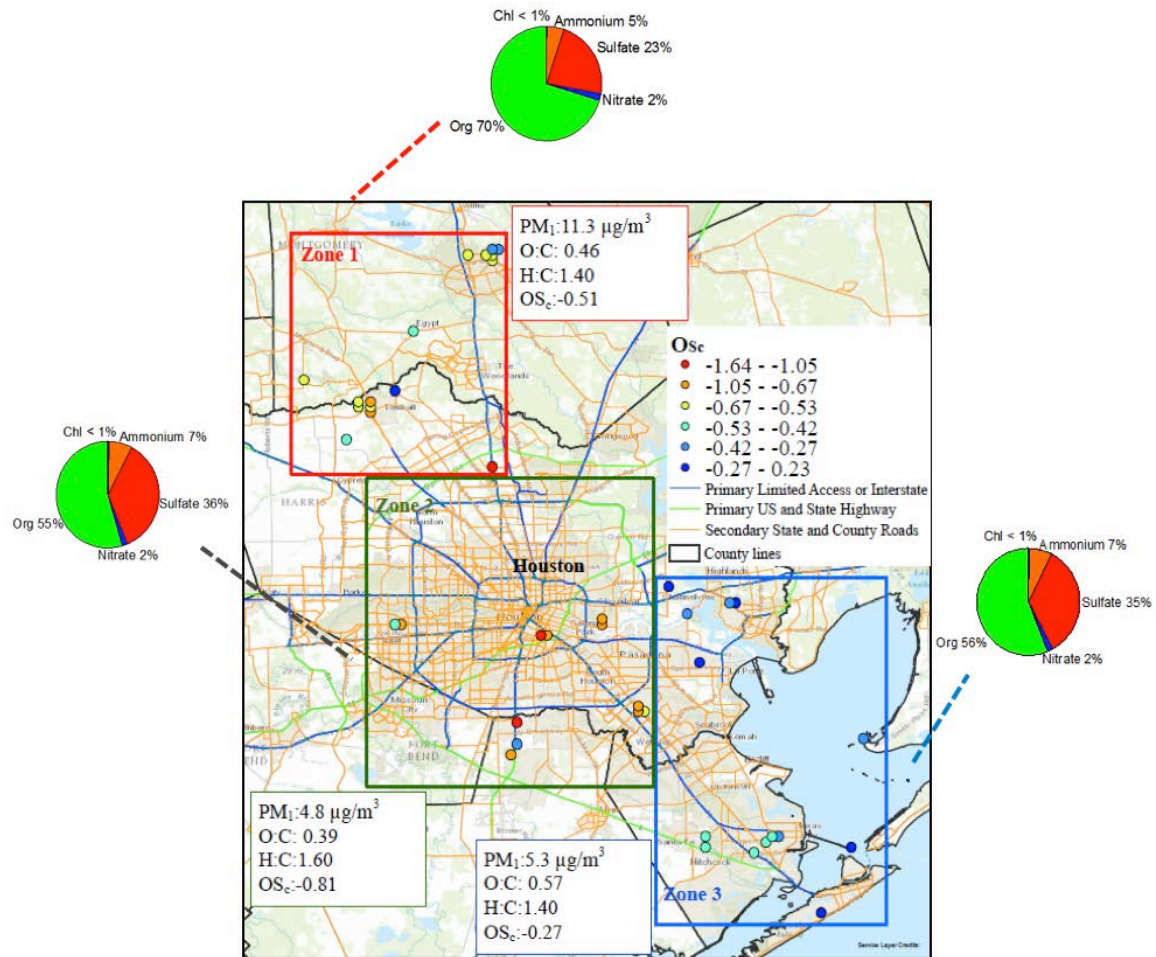
Figure 12. Average contribution of PM constituents, concentrations, and oxidation metrics in three analysis zones defined by OSc, OA concentrations, and geography.

Zone	OA	Sulfate	Nitrate	Ammonium	Chloride
1	8.16 (±3.54)	2.4 (±0.60)	0.23 (±0.15)	0.53 (±0.15)	0.019 (±0.007)
2	2.68 (±1.73)	1.68 (±1.01)	0.08 (±0.09)	0.37 (±0.26)	0.013 (±0.008)
3	3.03 (±1.9)	1.58 (±0.63)	0.08 (±0.047)	0.33 (±0.16)	0.0076 (±0.004)

Table 3. Average concentrations ($\mu g\ m^{-3}$) and associated standard deviations (in parentheses) of PM species in the defined analysis zones.

Results and Discussion – Task 5

Task 5 focuses on more specific determination of OA oxidation state and similar metrics during the campaign. In addition to the application of factor analysis by PMF for identification of aerosol components (e.g., HOA and various forms of OOA) (Ulbrich et al., 2009), the feasibility of conducting a three-dimensional (3-D) factorization technique, specifically parallel factor analysis (PARAFAC), has been evaluated. The extension of the two-dimensional analysis (PMF) to a 3-D analysis (PARAFAC) of size-resolved organic composition dataset has been reported only to a minimal extent previously.

The PMF analysis of the OA dataset generated during DISCOVER-AQ was conducted using PMF2 (version 4.2) running in robust mode. The main factors contributing to the organic fraction of the submicron aerosol were identified in a sub-dataset corresponding to the last two weeks of the campaign when concentrations were highest and data were most reliable and continuous. Results indicate that three main factors explain most of the variance in the dataset: a component corresponding to HOA and two OOA components (OOA-I and OOA-II). The identified factors agree with those reported by previous studies. The degree of oxidation follows the order HOA < OOA-I < OOA-II, with m/z 44 constituting 3.5, 7 and 12% of the MS signal, respectively. The average mass spectra of the three factors are given in Figure 13. The average relative contribution of these factors to total OA mass during the last two weeks of the campaign are 18% (HOA), 63% (OOA-I), and 19% (OOA-II), respectively, indicating that locally produced SOA contributes a significant fraction to PM OA mass in Houston. As an example, time series of each of these factors over a short period in late September are exhibited in Figure 14.

Several standard quality control checks were performed on the PMF solution. Fitting residuals were reasonable based on final fitting parameters and convergence criteria. The time series of the concentrations of each PMF factor were compared against internal (HR-ToF-AMS) and external (trace gas) tracers for reality checks. It was found that the HOA factor co-varied with primary combustion tracers such as CO and NO_x (Pearson R values of 0.45 and 0.44, respectively). Co-variance also was observed between the locally produced, secondary OOA-I factor and HR-ToF-AMS nitrate signal (R = 0.79). The nitrate signal has been related to organic nitrates. This also is supported by reasonable correlation between OOA-I and an HR-ToF-AMS nitrogen-containing organic MS fragment (R = 0.37). As such, there is reasonable evidence that OOA-I in Houston is at least partially associated with organic nitrogen-containing particles generated from nitrate radical- or hydroxyl radical (OH)/NO_x- initiated chemistry. Finally, the OOA-II signal shows weak but possible co-variance with aged parameters such as odd oxygen and AMS sulfate (R of 0.53 and 0.67, respectively). The data would likely show even better correlation when segregated by space, time, and other parameters as this would avoid inconsistencies caused by changes in meteorology on the smaller scale and the assumption of a constant MS for each factor across time and space, as discussed subsequently.
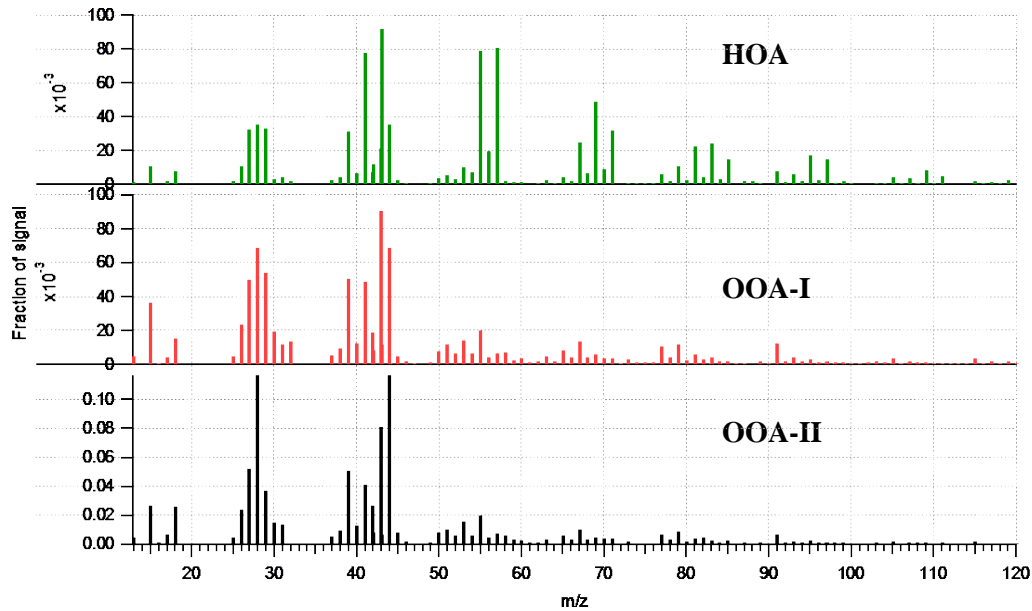
Figure 13. Average MS of PMF factors in OA during DISCOVER-AQ. HOA (green) represents POA, OOA-I (red) represents fresh SOA, and OOA-II (black) represents aged SOA.
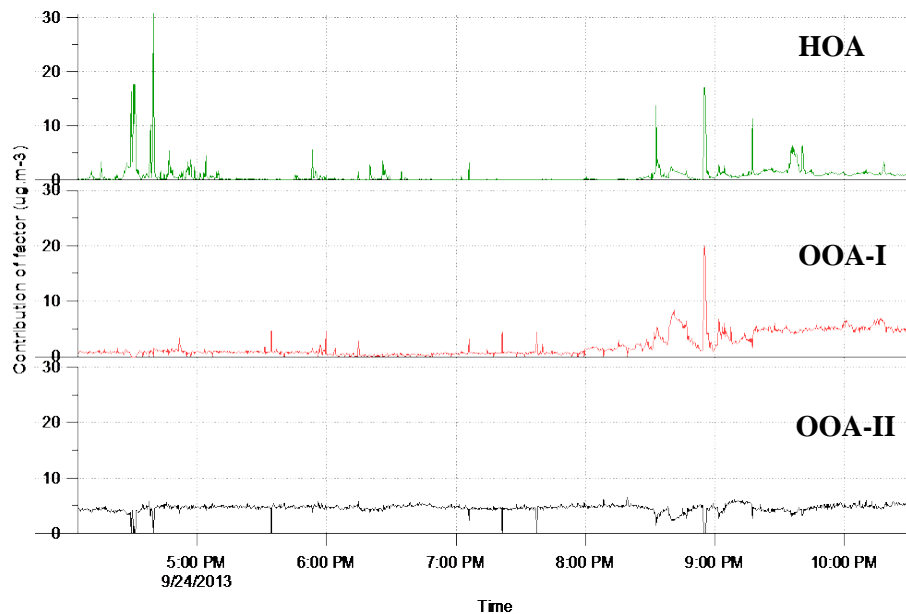
Figure 14. Time series of factors identified by PMF in submicron OA during DISCOVER-AQ. Only a short period on September 24, 2013 is shown as an example.

The PMF model assumes that MS patterns for each physical factor remain constant with time. The MS patterns for the three-factor solutions in each week individually show similar MS patterns, as well as similar values and consistent trends in

elemental analysis parameters (e.g., H:C and OSc). The differences between the two sets of PMF solutions at all m/z (up to 120) are relatively small.

Diurnal concentration profiles of these PMF factors provide broad information about the characteristics and sources of each factor in Houston. The HOA factor exhibits a strong morning rush hour (7:00-10:00 CDT) peak and several weaker peaks, indicating significant sources of fresh POA throughout the day in Houston. On the other hand, the more locally produced SOA factor (OOA-I) shows strong diurnal character, with elevated concentrations during night time. This diurnal profile suggests that a large portion of the less-aged SOA factor is produced by nitrate radical oxidation of volatile organic compounds (VOCs) and is less dependent on synchronous photochemistry. The proposed nitrate radical chemistry source of OOA-I is supported by a similar diurnal night time enhancement in nitrate. The elevated night-time concentrations could also be due to lower temperatures and the semi-volatile nature of the OOA-I factor. Lower temperatures allow the partitioning of semi-volatile species into the particle phase. The OOA-II factor, however, shows strong enhancement during daytime hours, likely due to the dependence of aging and growth processes on photochemistry. The diurnal characteristics described here provide strong validation of the PMF factors resolved from HR-ToF-AMS OA measurements, allowing further characterization of both primary and secondary sources of OA in Houston.

It should be noted that a combination of stationary and mobile measurements were included in the PMF analysis and that the method is still capable of separating the POA and SOA factors with reasonable fit residuals. The evaluation of co-variance with external tracers, diurnal variation, and spatial variation of the PMF factors validate this method of combining both stationary and mobile datapoints. Mean and median values follow similar trends in the diurnal profiles of the factors; thus, spatial diversity in the dataset (for both mobile and stationary measurements) is not expected to greatly bias the qualitative diurnal interpretations. Analysis of the spatial distribution and relative contributions of these PMF factors is presented below.

The spatially based average concentrations of each PMF factor in Houston can be found for the last two weeks of the campaign by dividing and averaging into square kilometer cells as was done for OA and other inorganic constituents previously. Average HOA concentrations were elevated on major freeways travelled by the MAQL (e.g., Interstate-10, Interstate-45, and TX-1488) and near point source industrial emitters. There are two regions in Houston where the OOA-I signal is relatively high: 1) in northwestern Houston where significant biogenic VOCs (BVOCs) could contribute to SOA production and 2) in southeastern Houston where elevated concentrations of reactive anthropogenic VOCs are expected to produce SOA. The distribution of OOA-II concentrations in Houston indicates that aged OA is elevated in the northwestern part of Houston and parts of central Houston, both of which are likely due to aged outflow from the city and industrial areas.

Similar methods can be used to determine the spatial distribution of the relative contribution of these PMF factors (that is, a fractional value after normalization by total OA). The HOA signal dominates on most freeways, while the locally formed OOA-I factor is ubiquitous (on average, 53% of total signal) throughout Houston, except regions where primary HOA dominates. Finally, OOA-II contributions to total OA are important

only in regions where both HOA and OOA-I concentrations are low. These observations indicate that all three PMF OA factors have distinct sources that are spatially variable in Houston. The distribution of the fractions of POA (HOA as a proxy) and SOA (sum of OOA-I and OOA-II as a proxy) to total OA mass has been analyzed similarly. It also should be noted that identical analyses performed using median values instead of mean values produced similar patterns, indicating that the observed concentration patterns are not greatly biased by extreme events and vehicular plumes.

The specific character (i.e., primary vs. secondary) of the OA and its diurnal variation was investigated in the statistically defined analysis zones for the Houston area (Zone 1- northwest Houston; Zone 2 - greater central Houston; Zone 3 - east and southeast Houston). This was performed based exclusively on stationary-mode measurements collected using the HR-ToF-AMS. The zone-based variation of the fraction of POA and SOA represented by the HOA and the sum of the OOA-I and OOA-II factors obtained by PMF analysis has been calculated. The dominant secondary character of OA in northwest and southeast Houston (Zones 1 and 3) is observed, with SOA representing an average of approximately 93% of OA. The OOA-I factor is more important than the OOA-II factor in these zones (62 and 57% of SOA for Zone 1 and 3, respectively). The OA in central Houston has a more primary character compared with Zones 1 and 3, although the average composition of OA in this zone still indicates the very important contribution of SOA (67%). The variation of the character of OA in Zones 1 to 3 suggests that different sources and processes determine the levels of organic PM across Houston, with the central part of the Houston area being more impacted by sources of primary aerosol (e.g., traffic activity) and northwest and east/southeast Houston being influenced by regional transport and VOC emissions (from biogenic and anthropogenic origin) leading to the formation of SOA. Though Zones 1 and 3 exhibit a similar apportionment of the OA, the source of the VOCs participating in the formation of this aerosol fraction is likely different due to different land uses and emissions point sources. This needs further study.

The diurnal variation of the HOA, OOA-I and OOA-II fractions in Zones 1 and 2 has been evaluated. The diurnal variation of PMF fractions in Zone 3 was not considered due to limited data availability for this zone.

The fraction of POA in northwest Houston peaks at approximately 8:00 CDT (approximately 23% of OA) during rush hour and remains below 10% during most of the day and nighttime. The OOA-I fraction exhibits the highest levels at night and in the early morning, reflecting the trends for nitrate observed at the field sites during DISCOVER-AQ, supporting the idea of significant association between this fraction and organic nitrates. The OOA-II fraction shows a peak during the afternoon hours (13:00 to 18:00 CDT) corresponding to the period of increased photochemical activity.

The fraction of POA in the central part of Houston exhibits two clear peaks corresponding to the morning and evening periods of high traffic activity, during which POA constitutes approximately 30% of the observed concentrations of OA. The OOA-I fraction in central Houston shows a different trend than that exhibited in the northwest part of Houston, with less marked increase during nighttime. The OOA-II fraction displays two clear peaks at approximately 11:00 and 13:00 CDT with increasing levels at night followed by a decrease in the early morning.

The variation in the degree of oxidation of the OA and its PMF factors across Houston during DISCOVER-AQ was examined based on the H:C, O:C, and OM:OC ratios and the OSc. The H:C ranged between 0.8 and 1.8 (average of 1.5 ± 0.1) with higher values observed in the eastern part of Houston, indicating a predominantly reduced (likely primary) character of the OA in this region. The O:C ratio and OSc varied between 0.2 and 1.4 and -1.5 and 1.5 across Houston, respectively. Average values of 0.43 ± 0.13 and -0.62 ± 0.37 were observed for these metrics, with higher levels identified in south and southwest Houston. The larger O:C ratio and OSc levels suggest that SOA including different degrees of processing is the major component of OA in these areas. Varying extents of oxidation is consistent with previous findings determined based on functional analysis of OA collected on filters (Cleveland et al., 2012). Although the O:C ratio and OSc values exhibit a similar trend, larger gradients in the degree of oxidation of the OA are observed based on OSc, which agrees with previous reports indicating potential limitations of the O:C ratio in capturing changes in the oxidation degree of the aerosol, specifically regarding functionalization reactions occurring in the aging process (Kroll et al., 2011).

The OM:OC ratio varied between 0.5 and 2.5 (average 1.70 ± 0.19), with larger values observed in the south and southwest parts of the Houston area. As the OM:OC ratio increases with an increase in the oxidation degree of the organics in the aerosol, it is expected that this metric resembles the O:C ratio and OSc distribution across Houston. The levels observed for H:C, O:C, and OM:OC ratios during DISCOVER-AQ show good agreement with previous studies that reported levels varying between 1.4 and 1.9, 0.2 and 0.8, and 1.41 and 2.0 for these metrics, respectively (Canagaratna et al., 2015).

The H:C and O:C ratios and OSc of these factors are presented in Table 4, along with values reported in the literature for these metrics. As shown in Table 4, the average O:C ratio and OSc value for OA during DISCOVER-AQ concur with values observed previously for PMF factors extracted from OA data. Higher levels of O:C and OSc for OOA-II compared to OOA-I indicate that this factor corresponds to highly processed aerosol (low volatility OA, LV-OOA), while OOA-I can be considered as "fresh" SOA typically classified as semi-volatile OA (SV-OOA).

Factor	H:C	O:C	OSc	O:C literature	OSc literature
HOA	1.98	0.09	-1.80	0.06 to 0.1	-1.7 to -1.6
OOA-I	1.56	0.58	-0.40	0.52 to 0.64	-0.5 to 0
OOA-II	1.39	0.92	0.45	0.83 to 1.02	0.5 to 0.9

Table 4. Metrics of the degree of OA oxidation for PMF factors identified during DISCOVER-AQ and comparison with literature values (Canagaratna et al., 2015).

A PMF analysis on an OA dataset collected in Houston during August 2014 also was conducted for comparative purposes, and the resulting average mass spectra of the factors are shown in Figure 15. In this case, four factors were identified. These factors exhibit a less oxidized character than those retained for the DISCOVER-AQ sub-dataset, suggesting a significant variation of the OA oxidation state as a function of space and

time across Houston and highlighting the need for continued measurements of OA across Houston and for an extended period of time.
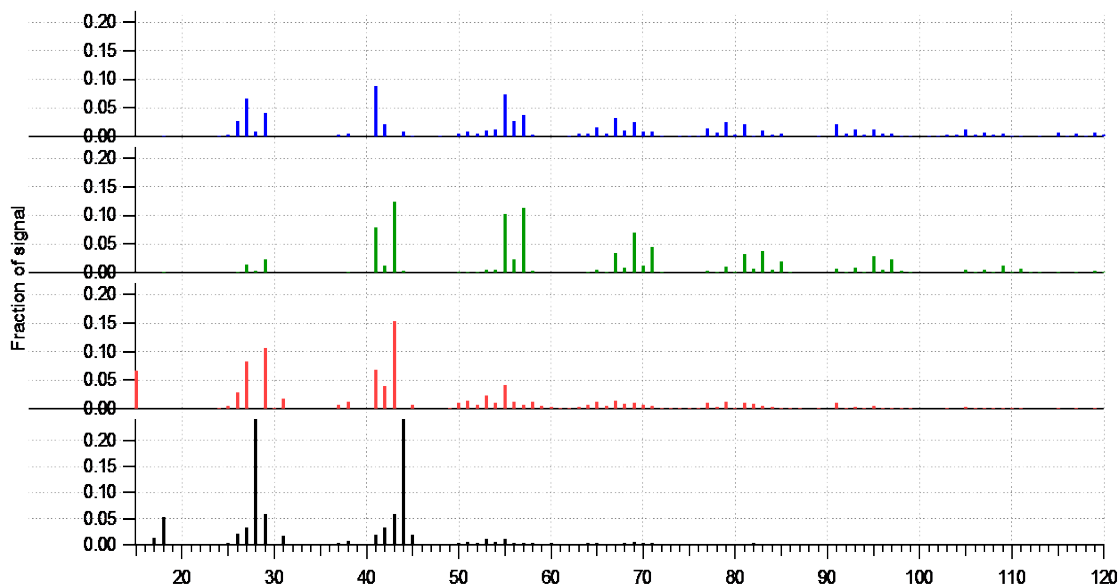
Figure 15. MS of factors identified in submicron OA in Houston during 2014.

Results and Discussion – Task 6

Task 6 focuses on understanding the importance of secondary processes with regard to PM formation in Houston. There is some overlap between Tasks 5 and 6, as the OOA components identified in PMF can be used as proxies for aged and fresh SOA, as described above. However, additional efforts have been made to identify other secondary processes of relevance to the PM measured as part of DISCOVER-AQ. The DISCOVER-AQ inorganic data have been formatted such that they easily can be input into freely available inorganic aerosol thermodynamic models; this allows estimation of the various forms of inorganic material present (for example, ammonium sulfate or ammonium bisulfate). This model output also includes aerosol liquid water content (LWC) and hydrogen ion concentration ($[H^+]$). It also is possible to compare precursor mixing ratios (such as those for SO_2) to corresponding particulate component concentrations (such as those for sulfate).

The ISORROPIA-I thermodynamic equilibrium model (Nenes et al., 1998) was used with the inorganic PM (sulfate, nitrate, and ammonium) and meteorological (temperature, relative humidity (RH)) data collected during DISCOVER-AQ. Simulations indicated that the aerosol was acidic throughout the DISCOVER-AQ campaign, with slightly more acidity in southeast Houston. A second freely available inorganic aerosol model (E-AIM) was tested (Wexler and Clegg, 2002); results indicated consistent LWC values but vastly different predicted $[H^+]$ values compared to those found using ISORROPIA-I (leading to a factor of two difference in predicted pH). This discrepancy has been observed previously, but for the sake of this work, the values determined by ISORROPIA-I will be used.

Correlations between predicted aqueous-phase [H$^+$] and measured OA concentrations and estimated H:C and O:C ratios were investigated. These correlations were performed for the five specific locations at which the MAQL was stationary and for a specific time period (22-28 September 2013, the most polluted period of the campaign). Results indicate that OA concentrations had very strong, positive correlation with ISORROPIA-predicted [H$^+$] in all locations between 22-28 September (R=0.80) and specifically in Manvel Croix and Galveston for non-continuous data over the entire campaign (R=0.86 and 0.94, respectively).

The LWC calculated using ISORROPIA-I is plotted against OA based on time and date of measurement for each zone in Figure 16, Figure 17, and Figure 18. Figure 16(Zone 1) shows that the LWC exhibits large variability in the morning hours (overnight, midnight to 8:00 CDT) at the beginning and the end of the campaign for two specific OA levels (5 and ~15 μg/m^3, respectively). That is, there are large changes in LWC with no response in OA. Figure 17 (Zone 2) exhibits a similar phenomenon with overnight measurements at the beginning of the campaign at OA levels of 4-5 μg/m^3. Furthermore, Figure 16 and Figure 17 indicate that predicted LWC values reach an approximate maximum of 5 μg/m^3 for afternoon (includes data from 8:00AM to 4:00PM CDT) and nighttime (4:00PM to midnight CDT) measurements over the entire campaign. Figure 18 exhibits this same LWC maximum for afternoon and nighttime measurements for Zone 3, but it should be stressed that the amount of data in Zone 3 is small compared to that in the other zones. The strong estimated increases in LWC in Zones 1 and 2 during overnight/morning hours may be related to the deliquescence RH (DRH) of the particles. During morning periods when RH is the highest, the particle has likely surpassed its DRH. At this point, the particle takes up significant amounts of water, which explains the large LWC observed in Figure 16 and Figure 17. It is interesting that no response in OA levels is observed during these periods, indicating either that OA has no impact on LWC or that LWC is not needed for partitioning/formation of OA during these periods. Similar plots showing these relationships but with markers representing specific sampling location are shown in Figure 19, Figure 20, and Figure 21. Figure 19 and Figure 20 indicate that Conroe and Manvel Croix, respectively, exhibit LWC-OA relationships that vary based on date of sampling.

In addition to investigating these relationships for bulk OA, the PMF results can be used to create regressions between calculated LWC and different OA factors (OOA-I (also known as SV-OOA), OOA-II (also known as LV-OOA), and HOA). This is done based on available data in each of the three analysis zones. Regression parameters (R and slope) for each factor in each zone (Figure 22, Figure 23, and Figure 24) do not indicate strong relationships. In fact, the strongest correlation coefficients across all OA factors are for HOA in Zones 1 and 3 (R_{Z1}=0.41, m_{Z1}=0.50; R_{Z3}=0.53, m_{Z3}=0.51). Visual inspection of these figures, however, indicate that these relationships are driven by a relatively small number of data points, meaning that little credence should be put in these values, especially as HOA is representative of POA. Further visual inspection of the OOA-I (Zone 1, nighttime) and OOA-II (Zone 2, daytime) relationships show the potential for strong relationships if a small group of outlying points is removed from the regression.
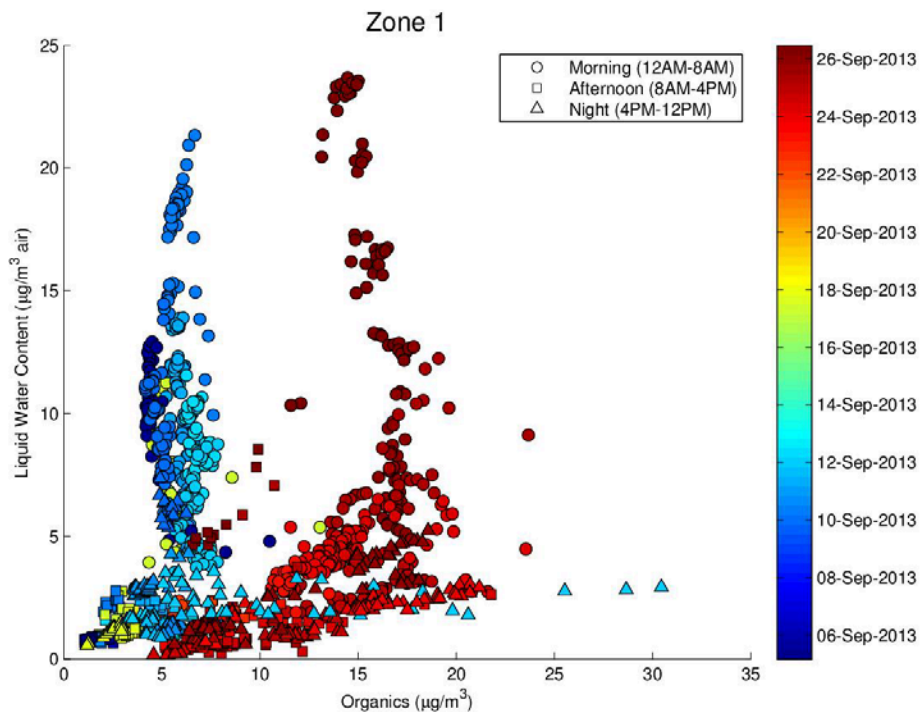
Figure 16. Scatter plot of LWC versus OA for Zone 1, where marker shapes represent time of day and marker colors represent measurement date.
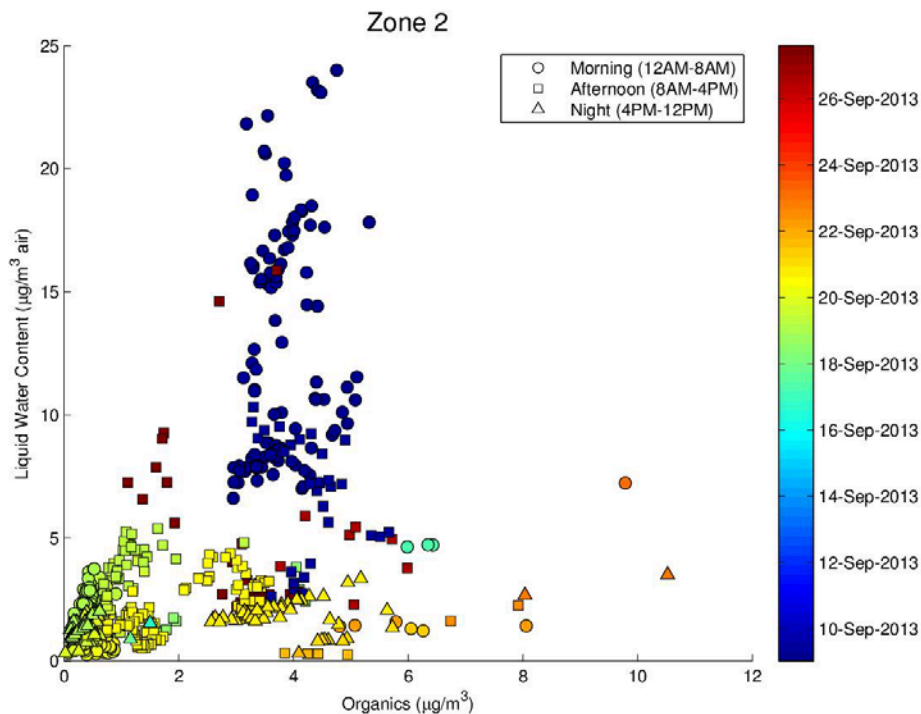
Figure 17. As in Figure 16 for Zone 2.
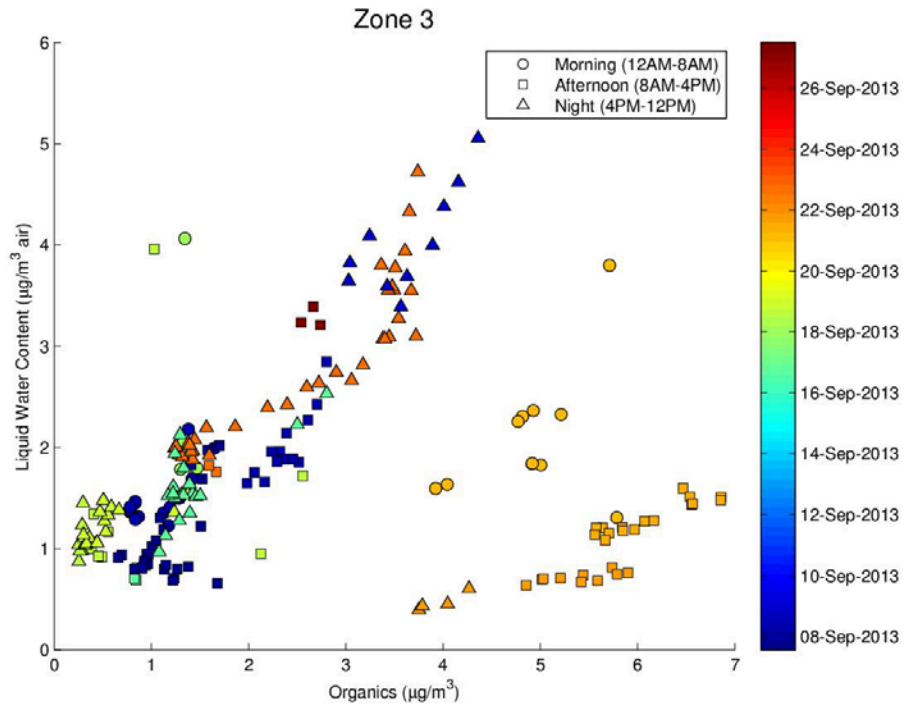
Figure 18. As in Figure 16 for Zone 3.
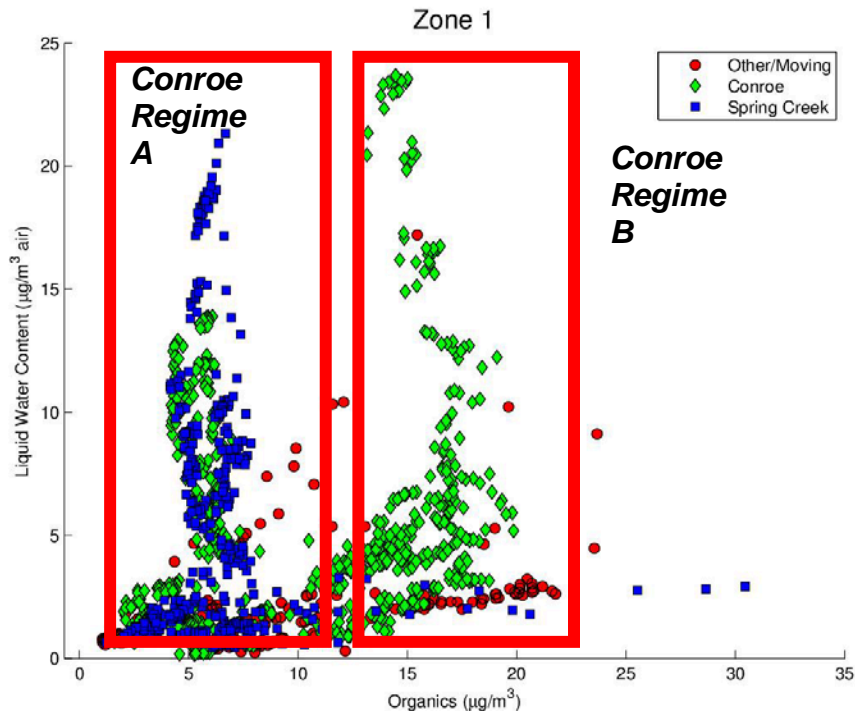
Figure 19. Scatter plot of LWC versus OA for Zone 1, where marker shapes represent
measurement location.
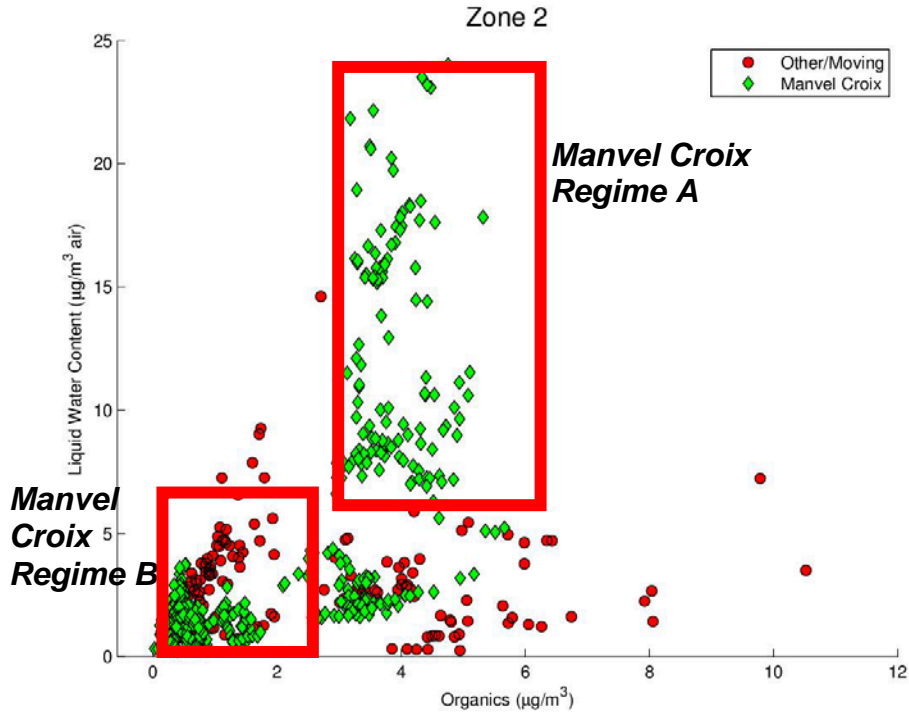
Figure 20. As in Figure 19 for Zone 2.
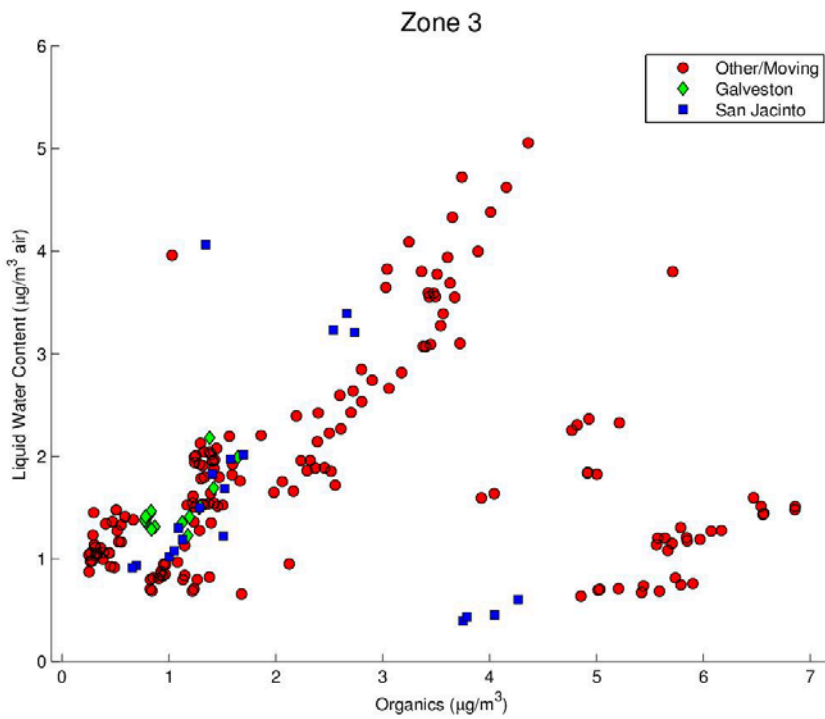
Figure 21. As in Figure 19 for Zone 3.
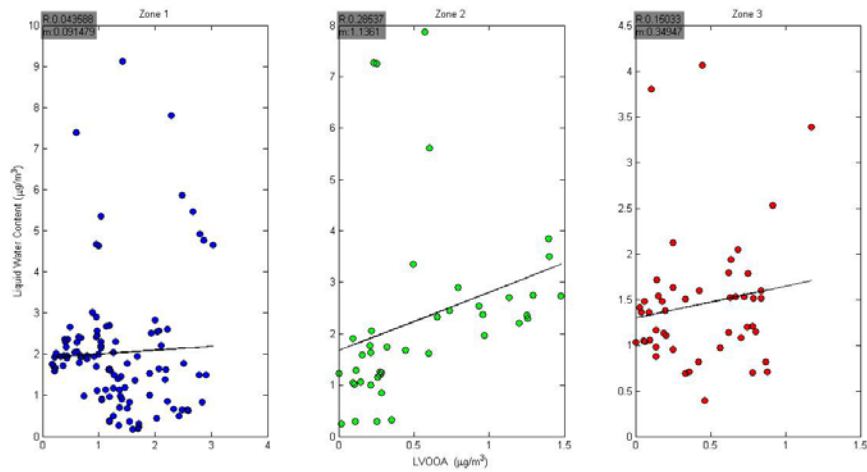
Figure 22. Regressions of LWC and LV-OOA for Zones 1 (Z1), 2 (Z2) and 3 (Z3). Parameters (R correlation coefficient, m slope): $R_{Z1} = 0.04$, $m_{Z1} = 0.09$; $R_{Z2} = 0.28$, $m_{Z2} = 1.13$; $R_{Z3} = 0.15$, $m_{Z3} = 0.34$.
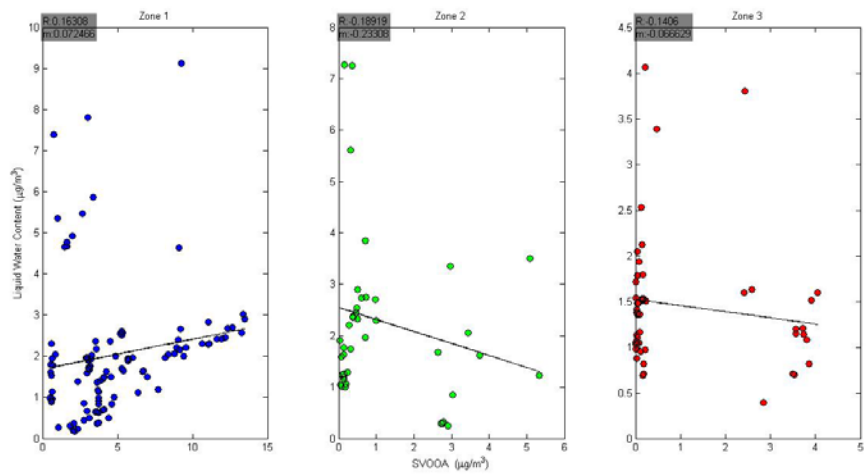
Figure 23. As in Figure 22 but for SV-OOA. Parameters: $R_{Z1} = 0.16$, $m_{Z1} = 0.07$; $R_{Z2} = -0.18$, $m_{Z2} = -0.23$; $R_{Z3} = -0.14$, $m_{Z3} = -0.06$.
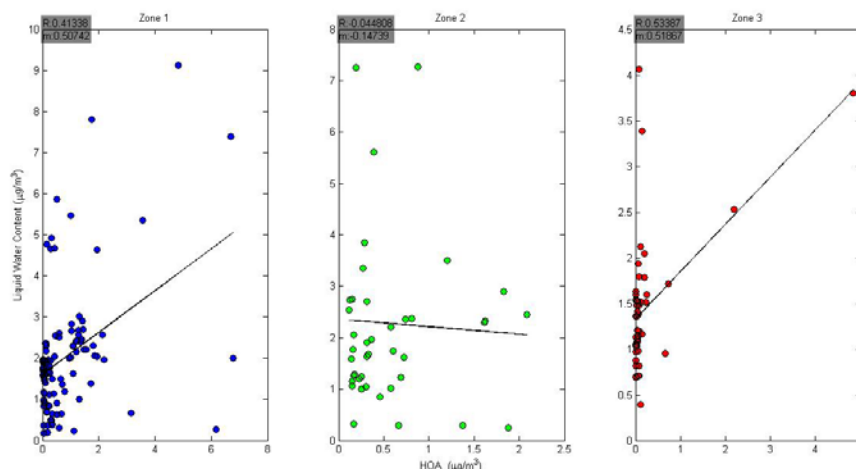
Figure 24. As in Figure 22 but for HOA. Parameters: $R_{Z1} = 0.41$, $m_{Z1} = 0.50$; $R_{Z2} = -0.04$, $m_{Z2} = -0.14$; $R_{Z3} = 0.53$, $m_{Z3} = 0.51$.

The association between ammonia concentration and the levels of sulfate and ammonium during DISCOVER-AQ were examined based on ammonia data provided by Dr. Mark Zondlo's group (Princeton University). Periods when the MAQL and the Princeton University mobile platform (PU-MP) were co-located were identified, and the spatial variation of the ammonia, ammonium, and sulfate concentrations during these periods was investigated. Expected similar trends for sulfate and ammonium levels are observed, but the association between ammonia and these constituents is not clearly identified due in part to the short period for which the mobile facilities were co-located. As a result, no conclusions regarding ammonia impacts can be drawn from these data.

However, the average spatial variation of the ammonia concentrations collected by the PU-MP during DISCOVER-AQ, and the spatial distribution of the ammonium, sulfate, and SO_2 concentrations obtained by the MAQL can be considered despite periods when the instruments were not co-located. In general, zones with high levels of ammonium and sulfate in PM do not correspond well to zones with particularly high levels of ammonia or SO_2. However, it is worth mentioning that the instrumentation also had different averaging times.

Further analysis on the degree of association between different trace gases, meteorological variables, and PM constituents was performed through generation of a correlation matrix. A weak correlation between SO_2 and sulfate levels suggests significant influence of regional transport on the observed sulfate concentrations.

Standard Principal Component Analysis (PCA) was applied in order to determine independent factors that contribute to the variance of the dataset comprised by aerosol constituents, meteorological variables, and concentration of different traces gases during DISCOVER-AQ. The PCA was applied on the entire dataset collected for the Houston area (HA) during the field campaign and on sub-datasets corresponding to the analysis zones previously defined (Zone 1 - Northwest Houston; Zone 2 - Central Houston; Zone 3 - Southeast Houston). Following PCA application, multiple-linear regression analysis based on the absolute principal component scores (APCS) of the retained PCA factors was conducted in order to determine their relative importance in explaining the observed

concentrations of PM during DISCOVER-AQ. In order to remove the correlation between the independent variable in the regression analysis (PM) and the dependent variables included in PCA analysis, the concentration of OA was removed from the dataset and a proxy for its oxidation state (O:C ratio) was included in the group of variables. Factors with eigenvalues in excess of one and jointly explaining at least 70% of the variance in each dataset were selected during PCA application, leading to four main components retained in each sub-dataset.

Table 5, Table 6, Table 7, and Table 8 present the loadings of the different variables in the retained components and the variance explained by each factor in each dataset. The four retained factors explain around 70% of the variance in the HA and Zones 2 and 3 datasets, while approximately 78% of the variance in the dataset corresponding to Zone 1 is explained by the selected PCA factors. Although the same number of factors was identified in each dataset, some variation was observed in the predominant variables in each factor. Table 9 summarizes the variables with large weights in each retained factor for the different datasets under analysis.

Rotated Factor Matrix

	Factor			
	1 (24.7%)	2 (18.3%)	3 (14.4%)	4 (12.2%)
O:C	.088	-.309	.220	-.103
NO_3	.667	.185	-.380	.334
SO_4	.965	.022	.137	-.033
NH_4	.974	.059	.057	.023
T	-.108	.131	.732	-.192
RH	-.118	-.026	-.810	-.121
CO	.143	.681	.027	.217
SO_2	.113	.727	.266	-.162
NO	.029	.852	.033	-.019
Isoprene	.016	.049	.531	.752
Terpene	.094	.067	-.292	.822

Table 5. Rotated PCA factors retained in the entire dataset (HA) for DISCOVER-AQ and percentage of variance explained (in parentheses). NO_3 = nitrate, SO_4 = sulfate, NH_4 = ammonium, T = temperature.

Rotated Factor Matrix

	Factor			
	1 (29.3%)	2 (21.7%)	3 (19.1%)	4 (8.3%)
O:C	-.562	-.019	-.412	-.268
NO_3	.665	.493	.191	.077
SO_4	-.088	.961	.015	-.080
NH_4	.105	.962	.049	-.032
T	-.883	-.106	.097	.182
RH	.869	.061	-.060	-.251
CO	.209	.237	.399	.586
SO_2	-.248	.073	.890	.091
NO	.118	.003	.910	.083
Isoprene	-.220	-.236	.033	.848
Terpene	.727	-.281	-.083	.206

Table 6. As in Table 5 but for northwest Houston (Zone 1).

Rotated Factor Matrix

	Factor			
	1 (32.6%)	2 (16.0%)	3 (11.9%)	4 (9.3%)
O:C	-.102	.083	.018	.851
NO_3	.053	.703	.435	-.144
SO_4	.278	.919	.032	.144
NH_4	.231	.938	.013	.108
T	.632	.138	-.115	.253
RH	-.540	-.151	-.502	-.296
CO	.734	.074	.028	-.083
SO_2	.699	.210	.075	-.070
NO	.790	.112	.009	-.145
Isoprene	.109	-.011	.871	.154
Terpene	-.193	.243	.686	-.272

Table 7. As in Table 5 but for central Houston (Zone 2).

Rotated Factor Matrix

	Factor			
	1 (21.0%)	2 (17.2%)	3 (13.8%)	4 (12.2%)
O:C	-.343	-.070	-.582	-.073
NO_3	.729	.199	.034	.458
SO_4	.017	.988	.030	.081
NH_4	.041	.983	.034	.083
T	-.927	.088	.102	.071
RH	.127	-.118	-.032	-.917
CO	-.054	-.013	.619	.225
SO_2	.253	.269	.425	-.122
NO	-.111	-.053	.840	-.002
Isoprene	.430	-.003	.201	.741
Terpene	.564	.077	.418	.011

Table 8. As in Table 5 but for southeast Houston (Zone 3).

Zone	F1	F2	F3	F4
Houston (HA)	SO_4 and NH_4	CO, SO_2 and NO	T, RH	Isoprene and terpene
1-Northwest Houston	T, RH and terpene	SO_4 and NH_4	SO_2 and NO	Isoprene
2-Central Houston	CO, SO_2 and NO	SO_4 and NH_4	Isoprene and terpene	O:C ratio
3-Southeast Houston	T and NO_3	SO_4 and NH_4	CO and NO	RH and isoprene

Table 9. Dominant variables in the retained PCA factors (F#) for the different datasets.

From these tables and the summary in Table 9, it is seen that Factor 1 in HA exhibits high loadings of sulfate and ammonium (secondary processes leading to PM formation), Factor 2 is dominated by CO, SO_2, and NO concentrations (anthropogenic emissions), Factor 3 is influenced strongly by temperature and relative humidity (meteorology), and Factor 4 exhibits high loadings of isoprene and terpene concentrations (biogenic emissions based on 3-D model output). The PCA factors in northwest Houston are related to biogenic emissions (Factors 1 and 4), with Factor 1 being influenced by meteorological conditions, secondary processes relevant to PM formation (Factor 2) and anthropogenic emissions (Factor 3). Retained factors in central Houston exhibit high loadings of CO, SO_2, and NO concentrations (Factor 1), sulfate and ammonium (Factor 2), and isoprene and terpenes (Factor 3). Factor 4 in Zone 2, which explains ~9% of the variance in the dataset, exhibits a high loading of O:C ratio and is the only variable with a significant weight in this factor. The PCA factors in southeast Houston exhibit high

loadings of NO_3 (Factor 1, which captures the NO_3 dependence on temperature), sulfate and ammonium (Factor 2), and CO and NO (Factor 3). The factors in Zone 3 seem to be less influenced by biogenic emissions, as only isoprene is dominant in Factor 4; it should be noted that the HSC is influenced by anthropogenic isoprene (Stutz et al., 2010).

The coefficients of correlation for multiple-linear regression analysis conducted based on APCS for the different datasets are presented in Table 10. Associated regression coefficients for each retained factor are also included in Table 10. Coefficients of correlation above 0.8 were observed for each dataset, indicating that APCS are suitable predictors of the PM levels. As the PCA factors are orthogonal (independent), the relative value of their regression coefficients provides an estimate of their relative importance in explaining the observed PM concentrations in each dataset. Accordingly, the influence of factors in PM concentrations in northwest Houston follows the order secondary processes (SO_2 to SO_4, NH_3 to NH_4) > biogenic emissions > anthropogenic emissions. Relative importance of factors in central Houston follows the order secondary processes (SO_2 to SO_4, NH_3 to NH_4) > anthropogenic emissions > biogenic emissions. The relative importance of PCA factors in southeast Houston follows the sequence secondary processes (SO_2 to SO_4, NH_3 to NH_4) > NO_3-related factor > anthropogenic emissions > biogenic emissions.

Zone	F1	F2	F3	F4	Constant	R
Houston	4.56	1.49	-0.219	2.41	4.012	0.86
1-Northwest Houston	2.42	3.01	1.45	1.92	8.011	0.80
2-Central Houston	1.51	3.45	1.19	0.17	0.48	0.91
3-Southeast Houston	1.83	1.93	0.32	1.04	10.1	0.93

Table 10. Results of regression analysis based on APCS for the different datasets.

Results and Discussion – Task 7

Task 7 evaluates the influence of BVOCs on O_3 and PM formation. To some extent, this was considered in the previous task when OOA-I concentrations were considered in the context of nitrate-radical induced oxidation of BVOCs in northwest Houston. Additional statistical analyses and modeling calculations are described subsequently. Because BVOC data are not available for the MAQL operation periods due to malfunction of the appropriate instrumentation, an alternative data source was identified as temporally and spatially resolved Community Multi-scale Air Quality (CMAQ) model output for isoprene and monoterpenes. The UH Air Quality Forecasting (AQF) group ran CMAQ simulations for every day during the campaign (as in Czader et al. (2015)). The model was run at a 4-kilometer spatial resolution with 1-hour time steps over southeast Texas. Isoprene and monoterpene data have been extracted for the MAQL locations during the month of September 2013. For this process, the CMAQ grid box was identified for each location reported by the MAQL GPS. The isoprene and monoterpene concentrations at the surface level were extracted for the closest model time step. The resulting time series shows an expected diurnal cycle with the largest peaks during the most polluted period of that month (September 25-26). Although there is no spatial overlap with the MAQL, isoprene data from a gas chromatograph on top of the Moody Tower during this time period provide an opportunity for a reality check on the

modeled data. When the model data are compared to this location, there is generally an underestimation from CMAQ, with the exception of the hottest and most polluted days of the month. However, in general, the diurnal patterns correlate with each other. This provides confidence that any effort to link modeled BVOC data to O_3 or SOA formation will do well temporally but likely will have uncertainty in terms of magnitude. Using output from Task 6, CMAQ BVOC time series will be considered versus time series of proxies for SOA. In addition, CMAQ BVOC time series will be provided for use in Tasks 9 and 10 to look at the influence of BVOC on O_3 and radical production.

To further investigate the processes leading to the formation of SOA in Houston, the association between BVOC levels and SOA concentration during DISCOVER-AQ was examined. Predicted levels of isoprene and monoterpenes were below 3 ppbv for the majority of the Houston area. Higher levels of these species were predicted in northwest Houston, with concentrations between almost 5 and 12 ppb. Based on the entire dataset, there were no statistically significant correlations between isoprene concentrations and SOA (sum of OOA factors), OOA-I, and OOA-II levels. A moderate degree of correlation was observed between monoterpenes concentrations and SOA and OOA-I levels ($R = 0.60$ and 0.65, respectively), while only a weak correlation was noted between monoterpenes concentration and OOA-II levels. The correlation between monoterpenes and OOA-I indicates that the formation process of OOA-I from monoterpenes is likely rapid, supporting the idea of nitrate-radical induced oxidation.

Considering the higher levels of isoprene and monoterpenes predicted for the northwest, correlations between concentrations of these species and SOA and OOA-I concentrations in Zone 1 were examined (using only stationary data). Monoterpene concentrations exhibit statistically significant moderate correlation with levels of SOA and OOA-I ($R = 0.50$ and 0.58, respectively). Correlation between isoprene concentrations and SOA, OOA-I, and OOA-II concentrations was not statistically significant. According to these results, monoterpenes are more likely to impact the formation of surface-level SOA in Houston (compared with isoprene) specifically the formation of the OOA-I fraction. This corroborates the theory presented earlier regarding the impact of monoterpenes on SOA formation through oxidation by nitrate radical, which also is supported by the results of the PCA described previously.

Results and Discussion – Task 8

Task 8 compares *in situ* surface NO_2 measurements with available Pandora NO_2 column measurements. Monthly averaged O_3 monitoring instrument (OMI) stratospheric NO_2 columns are subtracted from the Pandora measurements. Directly comparing surface concentrations to Pandora column measurements indicates a time-dependent relationship, with a larger slope during the middle of the day during peak periods of photochemistry. However, if the *in situ* NO_2 mixing ratio is integrated over the height of the boundary layer (from a Vaisala ceilometer CL31 LIDAR), the time dependence disappears, and the strength of this linear relationship improves ($R^2 = 0.53$), though the resulting slope of 0.41 indicates that assuming the NO_2 mixing ratio is constant up the boundary layer height is inappropriate.

Hourly averaged surface NO_2 also was integrated to the height of the boundary layer using a second profile shape: linearly decreasing to zero at the top of the boundary

layer. In urban Houston, the well-mixed profile assumption overestimates the boundary layer column. However, the linear profile decreasing to zero at the top of the boundary layer (a so-called half well-mixed column) improves this relationship. In less polluted Galveston, the errors in boundary layer height and the stratospheric subtraction cause larger scatter and yield a relationship more difficult to distinguish.

The Pandora spectrometer NO_2 data next were compared to the OMI satellite NO_2 measurements during DISCOVER-AQ. Cloudy conditions during this time period led to fewer data points for comparison than desired and expected. The OMI data were filtered by the row anomaly and cloud fractions greater than 20%. As recommended by Jay Herman (Pandora PI), Pandora data were only considered valid for clear sky direct-sun measurements, spectral fit root mean squared values less than 0.01, and NO_2 column measurement errors less than 0.05 Dobson units. Based on the valid data, the relationship between Pandora and OMI changes spatially in Houston, as observed in Figure 25. In some locations, the data cluster around the 1:1 line; in others, one technique consistently outputs larger OMI column concentrations than the other. The overestimation by OMI in rural sites is most likely due to the proximity of these sites to more polluted source regions that the larger OMI pixel is also sampling. Long-term Pandora data from the Moody Tower at UH give a larger dataset with which to compare to OMI. From March 2012 until August 2013, 86 valid comparisons show that Pandora measures larger vertical column densities on more polluted days. However, on cleaner days, the relationship seems to be scattered around the 1:1 relationship, as exhibited in Figure 26. The differences observed in Figure 25 and Figure 26 are likely due to the spatial scale differences and NO_2 spatial variability between the measurements because Pandora is a local vertical column measurement (~1km in the early afternoon) and OMI measures over a large area (13 x 24 km^2 at nadir).

The Pandora data were compared to a second retrieval for OMI NO_2 total column (KNMI DOMINO level 2 v2.0), as opposed to the NASA standard product (level 2 v2.1). Both OMI retrievals often yield lower column values than Pandora in heterogeneous regions with respect to NO_2 regions and higher ones in more rural/homogeneous regions. More rural areas, such as northwest Harris County or Galveston, often have OMI values larger than comparable Pandora measurements due to the large spatial footprint of OMI encompassing portions of the urban plume not local to the site.

The Channelview Pandora site is in a NO_x source transition zone, with strong sources to the southwest but fewer strong sources to the northeast. Due to the placement of the Pandora, the comparison depends on local meteorological conditions. In northeasterly winds, the Pandora is located in the relatively unpolluted portion of the pixel, leading to OMI measuring higher than Pandora; with southwesterly winds, the large urban plume from Houston and the HSC is advected over the Channelview measurement site, leading to a Pandora measurement that indicates a higher local NO_2 column compared to OMI.

The NO_2 mixing ratio also was measured *in situ* aboard the NASA P-3B and sensed remotely from the King Air B200 during the DISCOVER-AQ flights. For the flights, NO_2 measurements were compared to NO_2 column measurements from the Houston network of Pandora spectrometers when coincidences occurred. The Airborne Compact Atmospheric Mapper (ACAM) aboard the King Air B200 aircraft measured

NO$_2$ slant columns (nadir) from the aircraft altitude (~9 km). The instantaneous field of view for this instrument is reported as 0.35 km x 1 km. The ACAM slant columns are compared to Pandora slant columns and normalized over the range of that day's ACAM measurements to get a relative comparison. Analysis has been done only for September 25, 2013. The spatial footprint of the ACAM and Pandora measurements are much more similar than when Pandora data are compared to OMI data. The largest deviations from a 1:1 relationship (with ACAM being in excess of Pandora) are in the more polluted regions (Channelview, Moody Tower, Deer Park), likely due to the spatial heterogeneity of pollution leading to increased importance of the air-mass factor and might improve after conversion to an ACAM vertical column in the final product.

In order to compare Pandora measurements to P-3B data, the *in situ* data must be binned and integrated to produce a lower tropospheric column. The NO$_2$ mixing ratio was measured aboard the aircraft at one-second temporal resolution. Aircraft spiral data are averaged in 100-meter bins through the height of the profile and summed to derive a lower tropospheric column density. Data from above five kilometers are not available. Interpolation was used to fill in gaps of missing data. Profiles missing more than five bins were excluded from analysis. Coincident Pandora measurements were averaged through the time of the spiral. Aircraft data have information about the vertical distribution of NO$_2$, but the larger horizontal distribution of the spirals leads to the inclusion of areas not incorporated in the Pandora field of view. For this reason, the root-mean-squared error for this comparison increases with higher levels due to spatial variability and pollution. These results are shown in Figure 27.
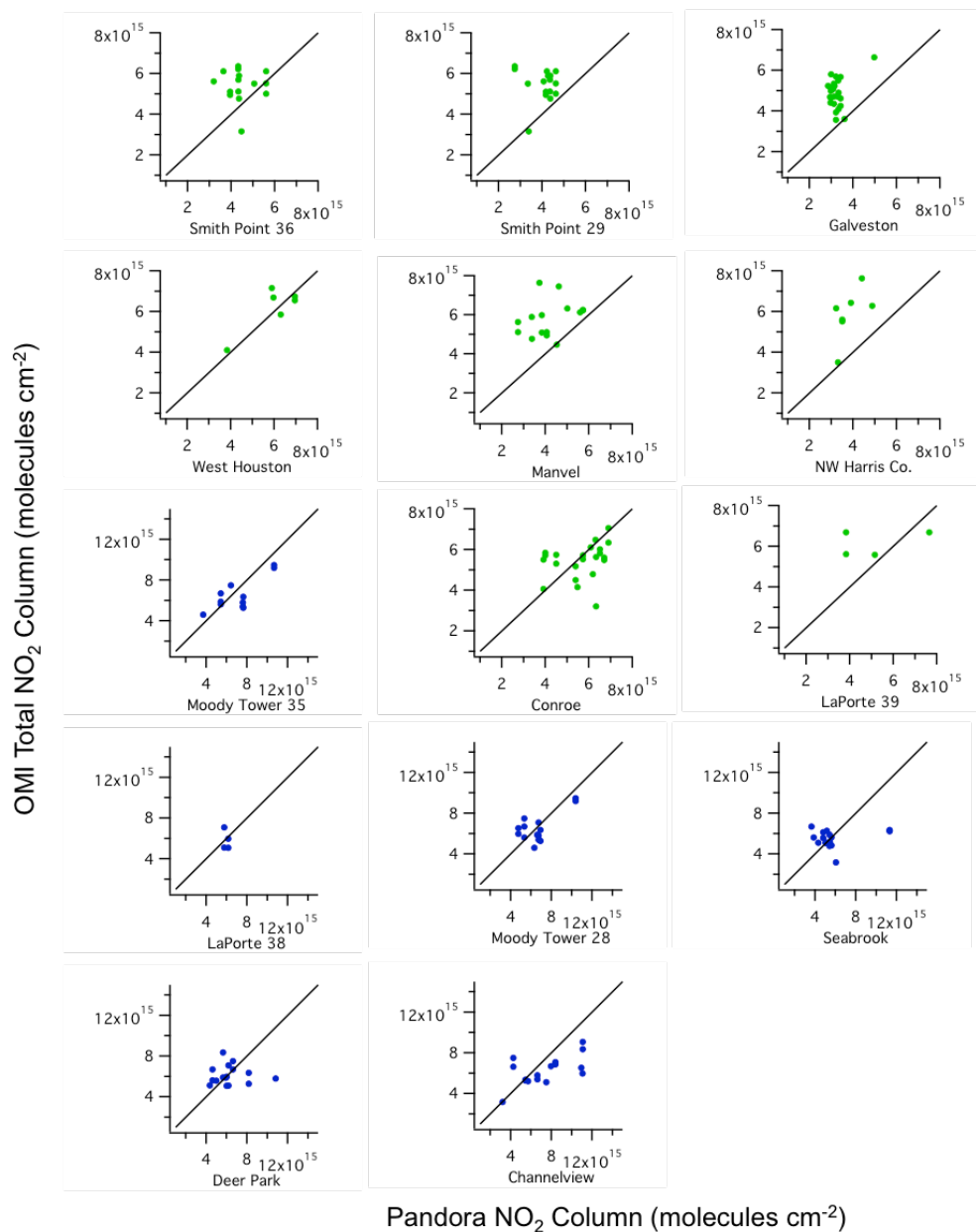
Figure 25. Comparison of OMI- (for the closest related pixel) and Pandora-derived (from specific ground stations) NO_2 columns across Houston during DISCOVER-AQ. Points are colored by scale used in the figure.
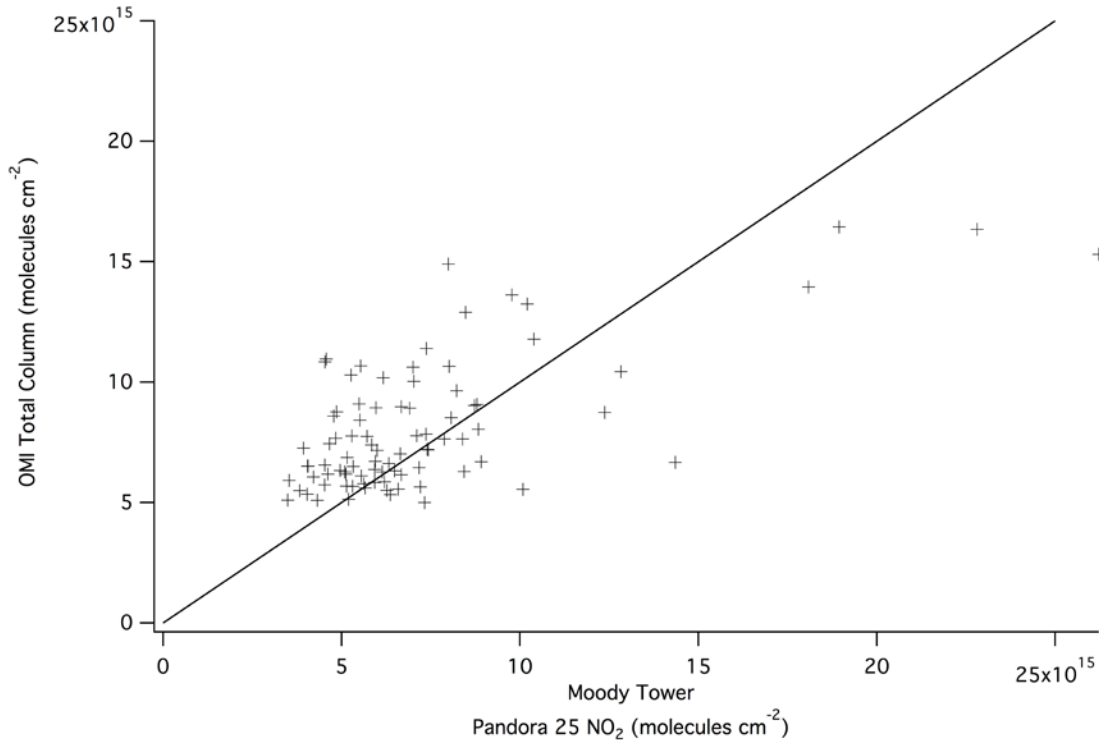
Figure 26. Comparison of OMI- (closest pixel) and Pandora- (*in situ*) retrieved NO$_2$ columns at Moody Tower for a more extended period of time.

Because previous work showed that the OMI satellite has a hard time capturing the spatial variability of NO$_2$ in an urban region, a new technique developed by Hyun Cheol Kim of the National Oceanic and Atmospheric Administration was applied to downscale OMI data to a finer resolution. This downscaling takes the OMI NO$_2$ mass for each pixel and uses CMAQ output to derive a spatial weighting kernel. The spatial weighting is then used to distribute the NO$_2$ measured by OMI at the CMAQ scale. The technique conserves NO$_2$ from OMI and does not distribute the mass outside the OMI pixel area. Downscaling has been applied in Houston and compared to DISCOVER-AQ Pandora and P-3B measurements. The CMAQ versions used include the 4-kilometer UH AQF model and the National AQF Center 12-kilometer model. To compare to the P-3B spirals, a weighted average of the OMI pixel or downscale grid boxes was taken, depending on how long the aircraft was located within each polygon. Only spirals within two hours of the OMI overpass were considered. Each Pandora measurement was matched to the OMI or downscale polygon in which it was located during that day. Clouds and the row anomaly from the OMI retrieval drastically limited data during the campaign, especially as flight days were not necessarily correlated with valid OMI retrievals. Most pixels from OMI were located on the edge of the swath.

Improvements in the HSC area (Channelview and Deer Park from the P-3B comparison) were expected, as OMI generally underestimated the NO$_2$ in that region. Results are shown in Figure 28. The downscaling technique distributed the expected NO$_2$ from the coincident pixels to bring the measurements from the P-3B into better agreement. The Pandora instruments did not observe this improvement. The different

footprints of the two measurements strongly impact the results. One Pandora measurement does not capture spatial variability, whereas the P-3B can measure the varying environments within the spiral area. The results in Conroe show a clear example where errors in model transport also can lead to a huge difference in the result. When modeled and measured winds agree, all aircraft, OMI, and downscale data are in good agreement. However, if model meteorology erroneously transports the Houston urban plume to the Conroe region, the redistribution was clearly incorrect.
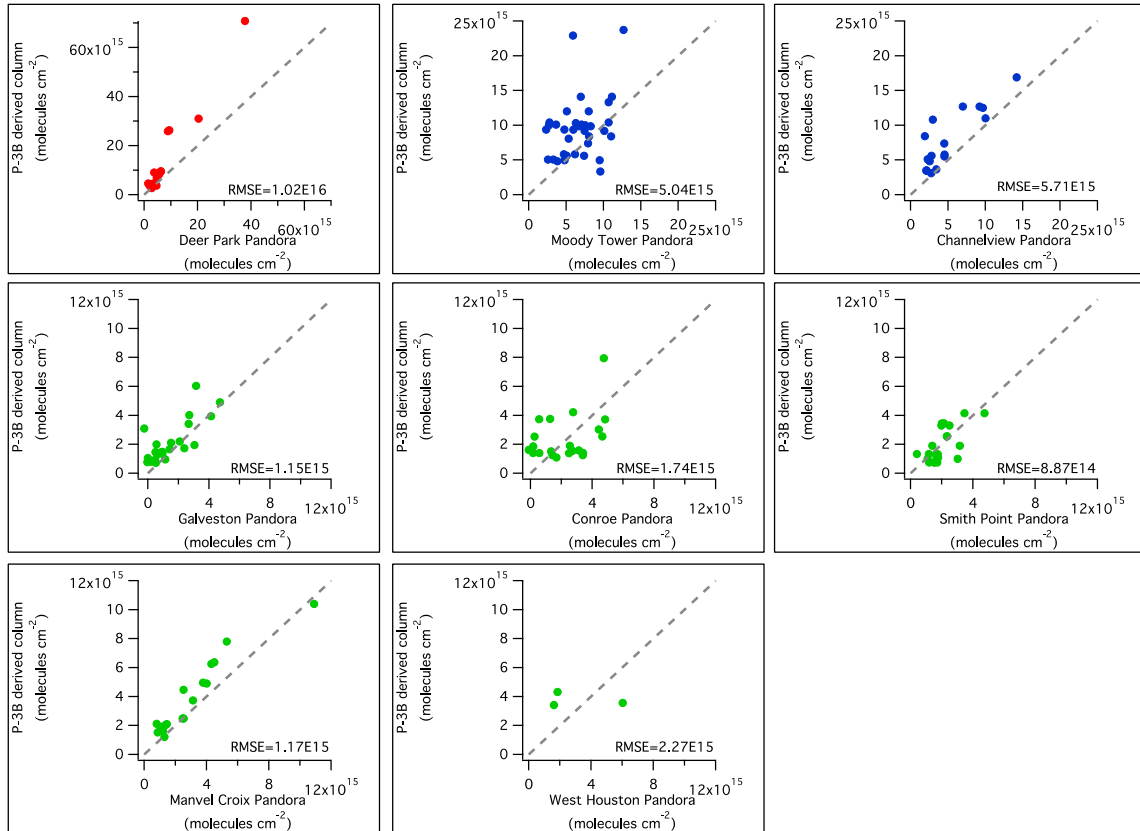
Figure 27. Comparison of aircraft- and Pandora-derived lower tropospheric NO_2 columns. Color indicates pollution scale (red most polluted, blue mildly polluted, green relatively unpolluted). Dashed lines indicate 1:1 relationships.
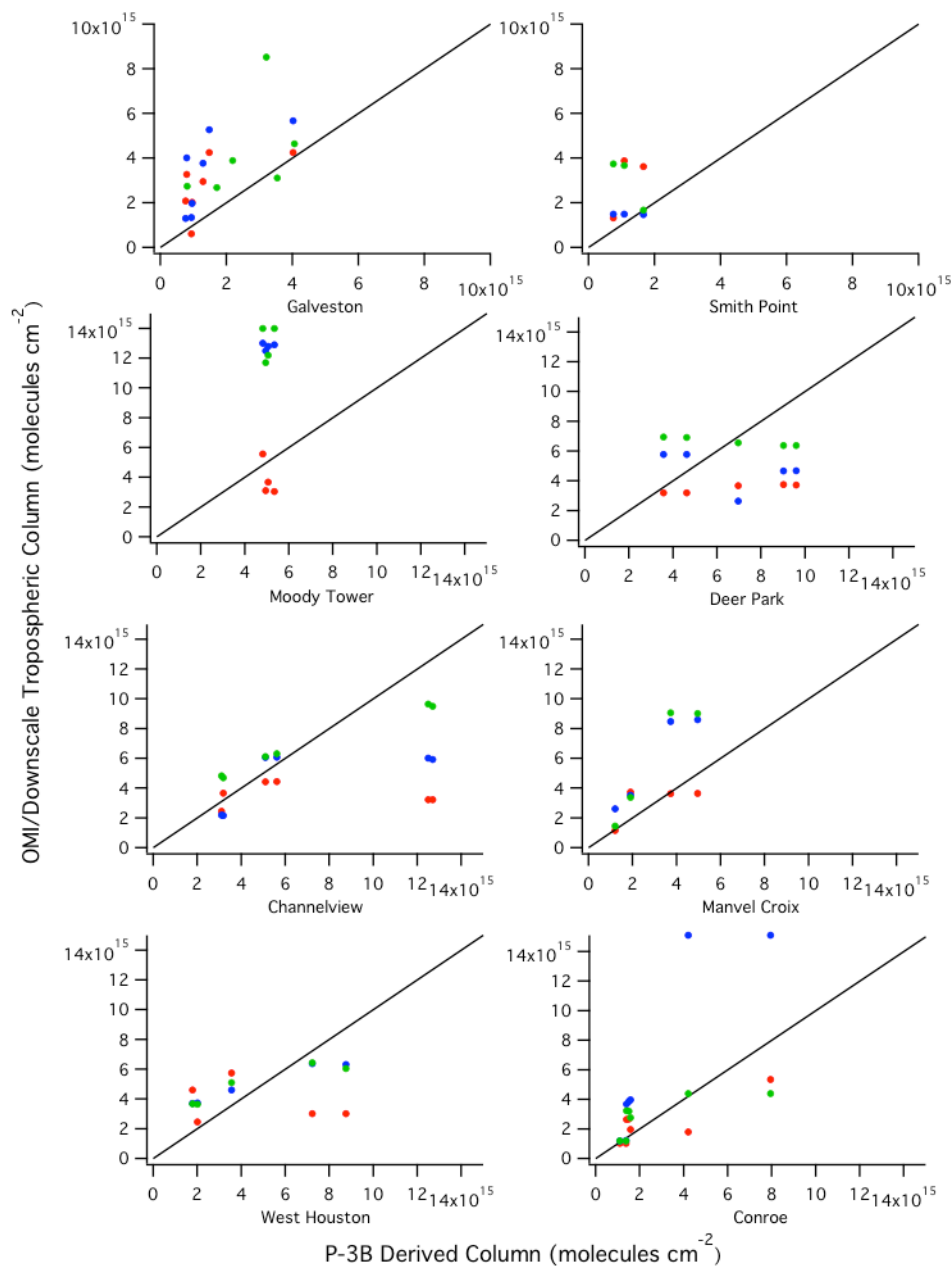
Figure 28. Scatter plots comparing the OMI- (blue: 4-km downscale, green: 12-km downscale) and P-3B-derived NO_2 columns at each spiral site.

Results and Discussion – Tasks 9 and 10

Tasks 9 and 10 use zero-dimensional computer modeling to evaluate O_3 production rates and radical sources (with a link to Task 7). Because the same modeling techniques are being used for each effort, the results of these tasks are combined for the sake of this report.

The NASA Langley Research Center (LARC) photochemical model was run with data from previous field campaigns to ensure that it was operating appropriately on a new

45

computational platform purchased for this effort. The LARC model ([Olson et al., 2006](#)) was run in a diurnal, steady-state, time-dependent mode. To solve for instantaneous values for O_3 formation and destruction, the model takes each time-step and runs input data through a diurnal cycle holding all constraints steady except for the photolysis rate constants (j values) and NO mixing ratio, which both change diurnally. Calculated values are accepted if convergence is within 0.5-1% of the initial starting point. From these values, formation (F), destruction (D), and net production (P) rates of O_3 are calculated. Previously published reaction mechanisms and kinetics are used. At a minimum, the model is constrained to O_3, CO, NO_x, methane, and VOCs. Model efforts will focus on two regions (Conroe and Manvel Croix) for which the largest amount of data (filtered to ensure modeling is not performed in motor vehicular plumes that titrate O_3) is available from the MAQL. The MAQL sampled for approximately three days at Manvel Croix, collecting 1081 data points for the model. At Conroe, the MAQL sampled for approximately ten days, gathering 4988 data points. Output will consider diurnal profiles.

The next step was to generate appropriate input files for the LARC model based on the MAQL data from DISCOVER-AQ. All required input data for the model (time, location, solar zenith angle, meteorology (temperature, dew point, and pressure), trace gas mixing ratios, O_3 column density from the NASA O_3 Mapping Profiler Suite, and the j_{NO2}) are available from the MAQL or other relevant sources, except the full suite of VOCs.

One method to determine appropriate VOC mixing ratios was to construct BVOC data from the CMAQ output discussed previously. A second method considered VOC data from Moody Tower and the P-3B (depending on which VOC mixing ratios were available). Moody Tower was used for ethane, propane, and other alkanes. The aircraft was used for formaldehyde, propene, benzene, and toluene. The VOC data from Moody Tower or P-3B spirals were regressed with either CO or NO_x data after sectoring by wind direction (to characterize different air mass source regions such as rural, urban, or industrial/urban). This allows the variation of the VOC within a wind sector to be based on overall pollution levels (as opposed to using a constant VOC to CO or NO_x ratio within a sector). The relationship for a source region was used when the MAQL was downwind of that region, and the measured CO or NO_x from the MAQL is used to estimate the corresponding VOC. The regression used within each sector (either CO or NO_x) was determined by regression parameters (that with the strongest correlation). This method was not used for BVOC, as there is not expected to be a relationship between BVOC and CO or NO_x, which typically are combustion tracers.

In the model, ethane, propane, ethene, benzene, ethyne, and isoprene are all treated explicitly. The rest of the alkenes, alkanes, and aromatics are lumped together into the three groups. Data from Moody Tower in 2010 was used to estimate the fraction of alkenes (propene), alkanes (butane, pentane, hexane), and aromatics (toluene) measured. When looking at Moody Tower data from 2010 with respect to the data measured during DISCOVER-AQ, 66% of alkanes were measured at Moody Tower, 55% of aromatics were toluene, and 48% of alkenes were propene. These ratios were applied to the estimations for total alkanes, alkenes, and aromatics.

Additional VOC scenarios were considered to investigate the influence of BVOC on O_3 formation in the two model locations. The scenario described previously is called the CMAQ scenario. A second scenario (ZERO) was investigated in which isoprene mixing ratios were set to zero. A final scenario (P-3B) was investigated by making any isoprene CMAQ value larger than the maximum value observed by the P-3B equal to the average P-3B spiral value at that location.

Results for the CMAQ case indicate that diurnal F and D rates for O_3 (and their individual components) peak just before noon at Conroe, as shown in Figure 29, Figure 30, and Figure 31, but show a significant drop around noon at Manvel (related almost exclusively to meteorology on one of the days simulated). Individual values calculated (in excess of 100 ppb per hour) are excessively large. Still, simulated O_3 formation from the reaction between hydroperoxy radicals (HO_2) and NO accounts for roughly half of the overall formation rate, regardless of time of day or location. Non-methyl organic peroxy radical (RO_2) reactions with NO account for roughly 37%, with methyl peroxy radical (CH_3O_2) reactions making up the remainder. This delineation is based on the regressions shown in Figure 32 for Conroe.

Figure 29. Average diurnal contributions of various routes of O_3 formation for Conroe based on measurements from the MAQL and CMAQ-derived isoprene mixing ratios.
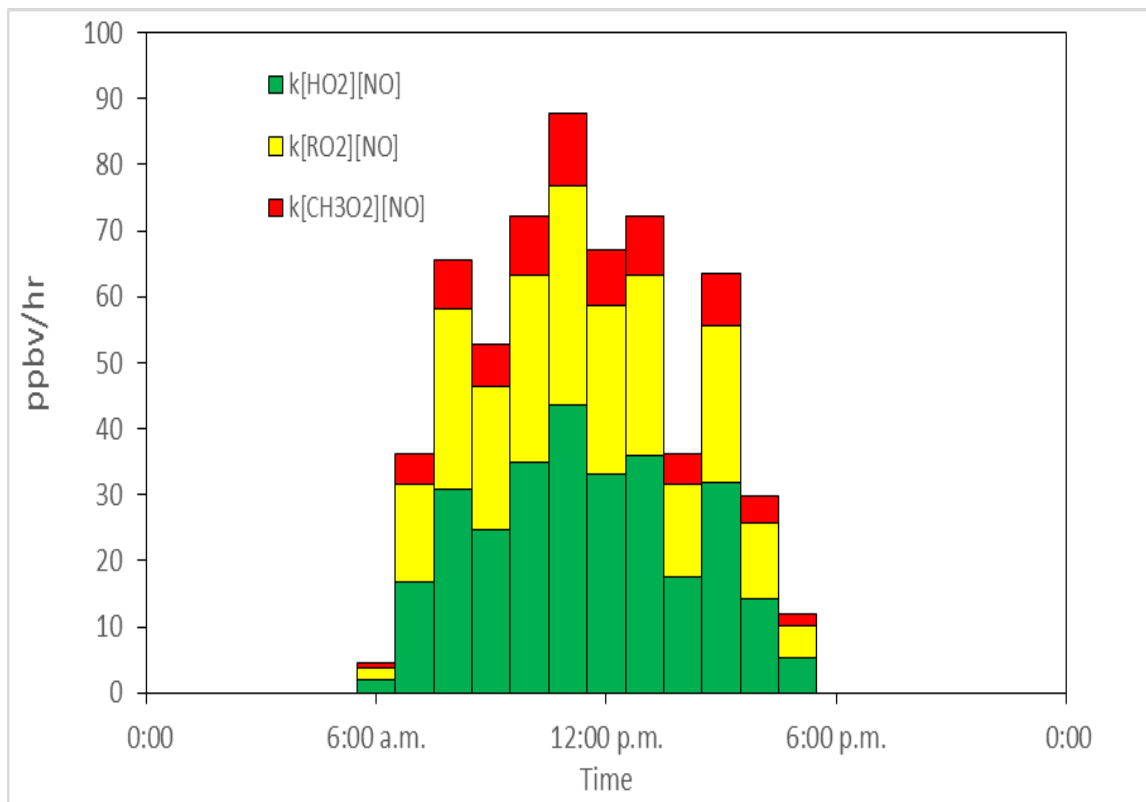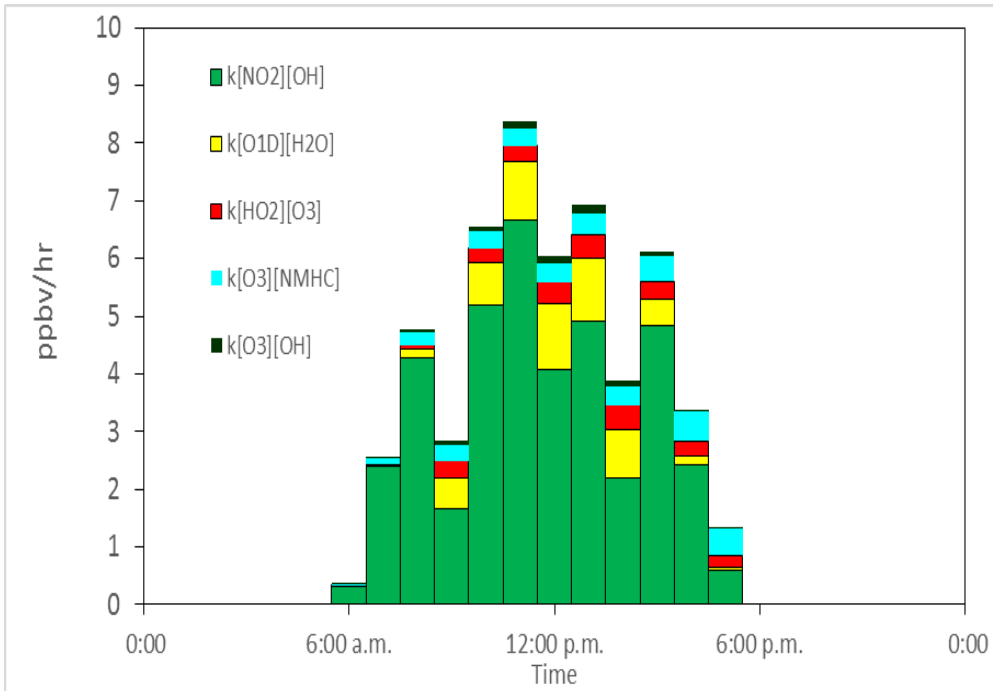
Figure 30. Average diurnal contributions of various routes of O_3 destruction for Conroe based on measurements from the MAQL and CMAQ-derived isoprene mixing ratios.
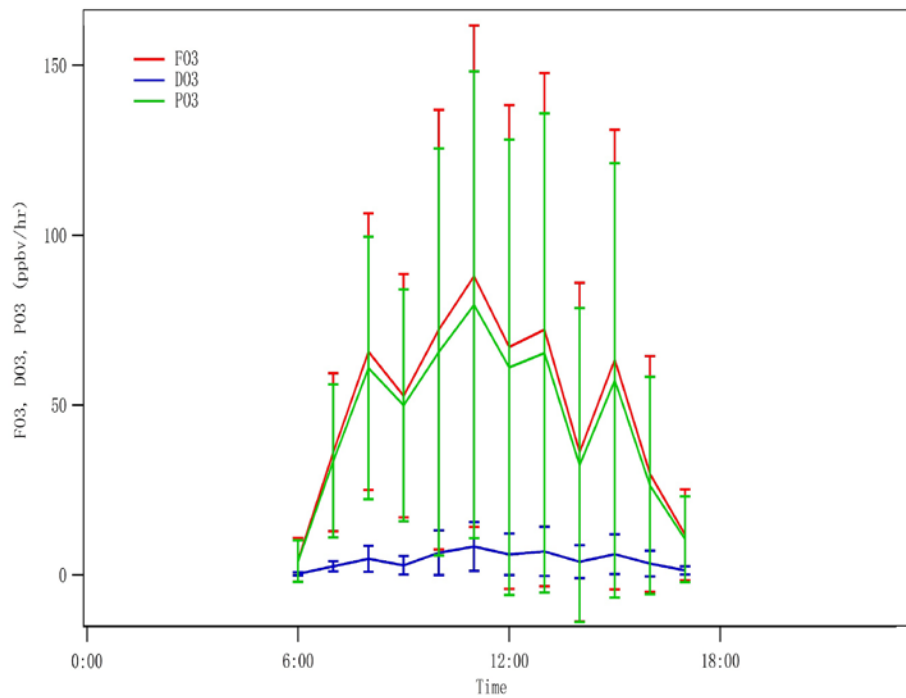
Figure 31. Average diurnal values for O_3 destruction (D, blue), formation (F, red), and net production (P, green) for Conroe based on measurements from the MAQL and CMAQ-derived isoprene mixing ratios.
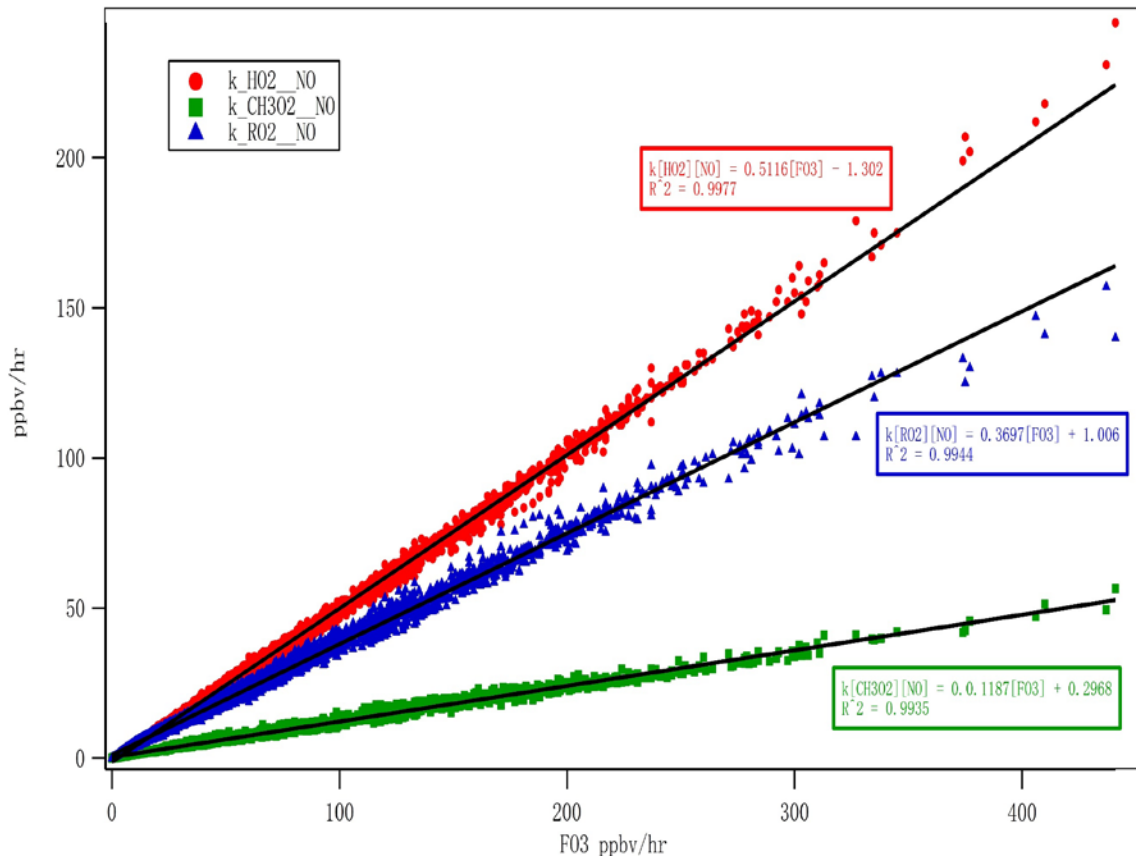
Figure 32. Regression of reactions rates versus O_3 formation rate where slopes indicate relative contributions of each rate to overall formations (HO_2, red; RO_2, blue; CH_3O_2, green). Values for Conroe based on MAQL measurements and CMAQ-derived isoprene.

In general during the day, F exceeds D, indicating a net positive P. Unlike the O_3 formation rates, however, the destruction rates of O_3 illustrate that the relative contribution of the individual rate components are more variable. At Conroe, D is dominated by HNO_3 formation, accounting for roughly 97% of the overall D rates. At Manvel Croix, D is dominated by HNO_3 formation only in the mornings, while losses due to specific O_3 reactions become more important in the afternoon. Generally, predicted F, D, and P values at Conroe are much higher than those at Manvel Croix, but similar overall results are observed between the two locations.

When P values are compared to levels of NO_x, as is done in Figure 33 for Conroe, both locations show the typical 'turnover' of P at higher concentrations, potentially indicating a transition between sensitive and saturated regimes with respect to NO_x. However, this transition is at a higher concentration than previously modeled in Houston.
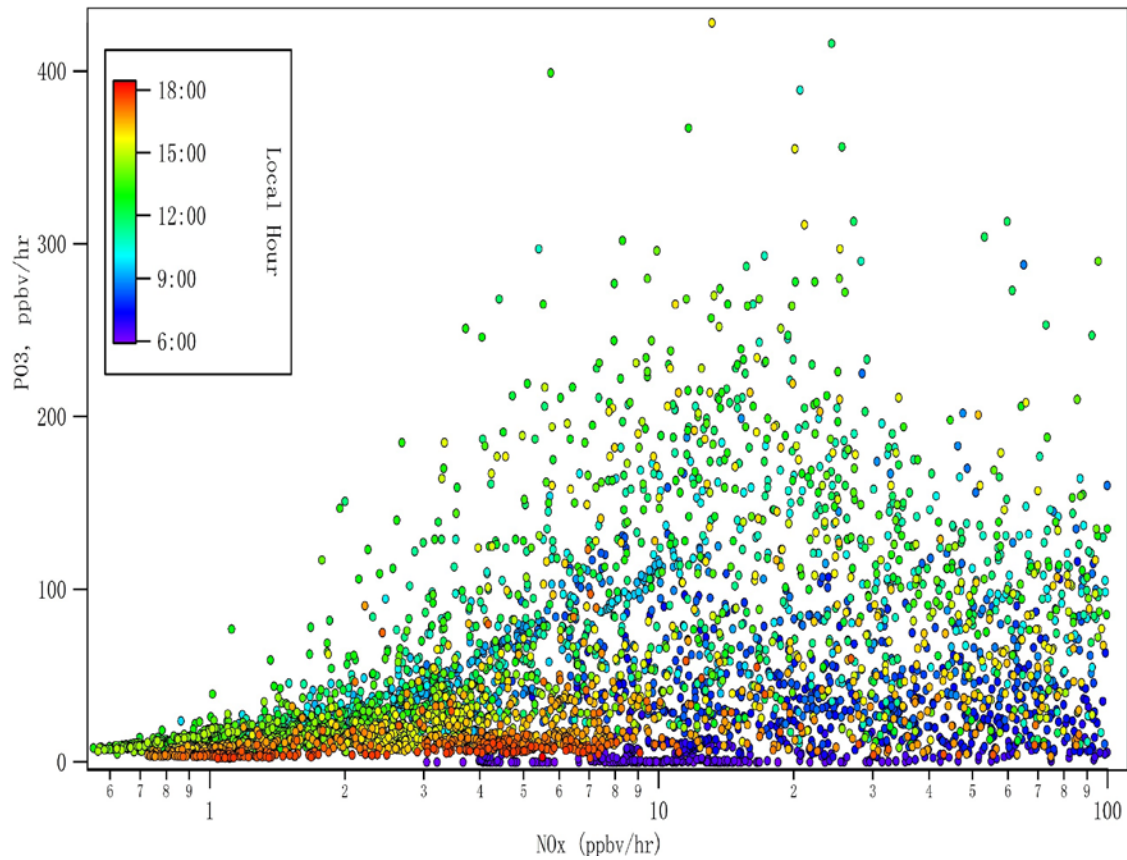
Figure 33. Net daytime O_3 production (colored by time of day) versus NO_x in Conroe based on MAQL measurements and CMAQ-derived isoprene. Only data with NO_x less than 100 ppbv are included.

For the ZERO scenario, observed rates are too small in magnitude to be realistic based on past observations but appear to have the appropriate diurnal profile. Conroe has a typical upwind diurnal pattern for F, D, and P for O_3. The peak around solar noon indicates that solar radiation is the driver for the diurnal pattern. In contrast, Manvel Croix exhibits a peak in the late morning due to its closer proximity to the urban and industrial source regions. This shows that the pattern in Manvel Croix is indicative of a balance between the NO_x and VOC morning emissions from rush hour and the increasing solar radiation later in the day. There is an exception around 1pm at Manvel Croix, which is caused by a decrease in solar radiation due to clouds during one out of the three days measured there (as discussed above).

Even in this ZERO scenario, both locations still exhibit the typical turnover of P, indicating a transition between NO_x-sensitive and VOC-sensitive regimes. This transition is still at a higher concentration than previously modeled in Houston. Manvel Croix also demonstrates how the pollution environment for O_3 production can change from day to day (based on meteorology) but seems to be mostly dependent on time of day.

As a quick test of the sensitivity of the LARC output to isoprene, the P-3B scenario was run. In this case, more realistic values of F, D, and P (net 20 to 30 ppbv per hour) were found at each location diurnally. Interestingly, the relative importance of

various contributors to F and D did not change relative to the CMAQ case (for both the ZERO and the P-3B cases). This indicates that O_3 formation in the Houston region is influenced strongly by biogenic activity, with isoprene influencing O_3 dynamics (but monoterpenes appearing to have a stronger influence on PM).

A fourth case was considered in which all VOC mixing ratios were corrected by P-3B data. This case is referred to as the P-3B-all scenario and will serve as the base case for the radical production investigation to follow. Data have been segmented by "traffic" and "non-traffic" periods based on location flags for the MAQL. Illustrative model output for Conroe is described here. The P-3B-all scenario leads to an expected diurnal profile for O_3 formation, with values for net $P(O_3)$ on the order of 20 to 40 ppbv per hour when away from periods associated with sunrise and sunset. These values are slightly higher when considering the traffic periods (for Conroe). The formation of O_3 is dominated by the reaction of NO with HO_2 and RO_2. The loss of O_3 is dominated by the reaction of NO_2 with OH to form HNO_3. Interestingly, the general trends and relative contributions of various pathways of formation and destruction do not appear to be very sensitive to the levels of VOCs used; rather, the overall magnitude of the rates depend strongly on these input values.

The P-3B-all scenarios at Conroe and Manvel Croix were used to approximate the most important relative contributors to the formation of HO_2. Within the LARC model, there are 69 non-photolysis chemical reactions and 15 photolysis reactions that can form HO_2. Table 11 and Table 12 list the relative contributions of the six main reactions contributing to HO_2 formation at Conroe and Manvel Croix, respectively. Here, precursors represent the related major species that form the reactants in the given reaction. For example, formaldehyde (CH_2O) is the major species that forms CHO that participates in Reaction 33. These results indicate that the relative importance of different pathways to HO_2 formation is quite consistent between Conroe and Manvel Croix. It should also be noted that Reaction 14 involving pernitric acid (HO_2NO_2) represents a rapid cycling between HO_2, NO_2, and HO_2NO_2 (also termed HNO_4); it is included for the sake of completeness.

Reaction Number	Percentage (%)			Reactants	Precursors
	Average	Non-traffic	Traffic		
14	35.9	39.1	33.7	HO_2NO_2	HO_2, NO_2
32	15.5	13.6	16.7	CH_3O, O_2	CH_3O_2, NO, CH_3OOH
33	15.1	14.4	15.5	CHO, O_2	CH_2O
8	8.7	8.2	9.0	H, O_2	OH, CO
68	6.6	5.1	7.6	ETO_2, NO	
91	6.3	6.9	6.0	RIO_2, NO	

Table 11. Average relative contribution to HO_2 formation of six main reactions and the related reactants at Conroe. Note that ETO_2 and RIO_2 are various forms of organic RO_2.

The destruction of HO_2 is caused by 29 chemical reactions in the LARC model. However, only two reactions account for the majority of HO_2 destruction, as shown in Table 13 and Table 14 for Conroe and Manvel Croix, respectively. It should also be noted that Reaction 13 involving HO_2NO_2 is included for the sake of completeness (as

above). Thus, HO_2 loss in these locations and periods is dominated by reaction with NO (to cycle to NO_2 and OH). Note that this does not represent a loss of total NO_x or of total hydrogen oxide radicals (HO_x) but highlights the importance of their internal cycling. Generally, the formation and destruction rates of HO_2 are larger during traffic-affected periods at Conroe (absolute values not shown), indicating the importance of NO_x in the cycling of HO_x at this location.

Reaction Number	Percentage (%)
14	32.7
32	16.5
33	15.9
8	11.4
68	5.2
91	4.5

Table 12. The average relative contribution to HO_2 formation of six main reactions at Manvel Croix.

Reaction Number	Percentage (%)			Reactant
	Average	Non-traffic	Traffic	
9	59.3	50.8	64.6	NO
13	36.1	40.0	33.6	NO_2

Table 13. The relative contribution to HO_2 destruction rate of two main reactions and the related reactant at Conroe.

Reaction Number	Percentage (%)
9	61.3
13	33.2

Table 14. The relative contribution to HO_2 destruction rate of two main reactions at Manvel Croix.

Using LARC model output, a similar analysis can be performed to identify various contributions of RO_2 to O_3 formation at Conroe and Manvel Croix. This also allows an inference of the importance of different VOC to RO_2. There are 21 chemical reactions between RO_2 and NO that are estimated to contribute significantly to O_3 formation. These results, similar to those shown above, appear in Table 15 and Table 16 for Conroe and Manvel Croix, respectively. Again, the reactants listed are those that participate in these reactions, and the precursors listed are those that lead to those reactants (e.g., PAN leads to MCO_3 in Reaction 171). Given that PAN and acyl radicals are derived from aldehyde chemistry, the results in Table 15 and Table 16 underscore the importance of aldehydes as well as BVOCs (isoprene). The influence of BVOCs decreases in traffic-related periods and in Manvel Croix relative to Conroe, as would be expected.

As above, using LARC model output, a similar analysis can be performed to identify various contributions to CH_3O_2 formation at Conroe and Manvel Croix. There are 23 non-photolysis chemical reactions and one photolysis reaction that can form CH_3O_2 in the LARC model. Table 17 and Table 18 show the major reactions that create CH_3O_2. It should be noted that Reaction 25 involving methyl peroxy nitrate ($CH_3O_2NO_2$)

represents a rapid cycling between CH_3O_2, NO_2, and $CH_3O_2NO_2$; it is included for the sake of completeness. Note that this does not represent a loss of total NO_x or of RO_2 but highlights the importance of their internal cycling. Thus, CH_3O_2 formation in these locations and periods is dominated by PAN and higher aldehyde chemistry. As would be expected, loss of CH_3O_2 is governed by reaction with NO.

Reaction Number	Percentage (%)			Reactants	Precursors
	Average	Non-traffic	Traffic		
171	29.9	28.2	30.8	MCO_3, NO	PAN, ALD2, OH
91	15.2	17.9	13.7	RIO_2, NO	ISOP, OH
68	14.4	12.1	15.7	ETO_2, NO	RCO_3, NO
121	11.9	10.3	12.7	RCO_3, NO	ALD3, OH, ISOPRD

Table 15. The relative contribution of the four most important reactions to total RO_2 + NO and the related reactants and precursors at Conroe. MCO_3 and RCO_3 are acyl peroxy radicals; ALD2, ADL3, and ISOPRD (from isoprene) are aldehydes.

Reaction Number	Percentage (%)
171	28.9
91	12.3
68	11.7
121	9.1

Table 16. The relative contribution of the four most important reactions to total RO_2 + NO at Manvel Croix.

Reaction Number	Percentage (%)			Reactants	Precursors
	Average	Non-traffic	Traffic		
25	68.6	72.9	65.4	$CH_3O_2NO_2$	CH_3O_2, NO_2
171	27.5	22.4	31.2	MCO_3, NO	PAN, ALD2, OH

Table 17. The relative contribution of the two most important reactions to formation of CH_3O_2 and the related reactants at Conroe.

Reaction Number	Percentage (%)
25	65.1
171	25.5

Table 18. The relative contribution of the two most important reactions to formation of CH_3O_2 at Manvel Croix.

Summary

All tasks have been completed within the timeframe of the project. A summary of the key findings for each of the tasks appears below; the subsequent section highlights future work, recommendations with respect to improvement of air quality in Houston, and concluding remarks.

Task 1 focused on characterization of on-road primary PM emissions by source in a size- and chemically resolved manner. Particle emissions generally occurred in the range of 100 to 200 nm in diameter, and the material was predominantly OA. Motor

vehicular emissions can lead to OA enhancements of up to approximately 70 $\mu g\ m^{-3}$. Depending on the vehicle type and methodology used, estimated EF values determined using the protocol developed here range from 0.14 to 13.74 g OA per mile driven.

Task 2 also focused on evaluation of statistically large, short-lived PM events and included both on-road and point sources such as petrochemical facilities and open burns. Large motor vehicular emission events are distributed between light-duty gasoline vehicles, light-duty trucks, and heavy-duty vehicles, and the resulting OA was reduced in nature. The sampled BB events lead to enhancements of OA (also chemically reduced in general) in excess of 100 $\mu g\ m^{-3}$. Large sulfate enhancements were observed near petrochemical facilities near flaring operations and storage tanks.

In contrast to the efforts described above which focused on short-term events, Task 3 focused on the typical diurnal profiles of PM across Houston. Diurnal profiles (in terms of both magnitude and exact temporal dynamics) are variable across Houston locations sampled. Generally, nitrate increased at night, sulfate and ammonium co-varied and were relatively flat, OA increased significantly during rush hours, and OA exhibited moderate afternoon increases related to a deep boundary layer coupled with photochemical formation of SOA.

Similar to Task 3, Task 4 considered broadly PM across the region by determining the typical composition of PM across Houston. Across Houston, the dominant components of PM are, in order, OA, sulfate, ammonium, nitrate, and chloride. In Galveston at the site used, sulfate contributes more to mass than OA. The relative contribution of OA increased when moving from southeast to northwest.

Because of the importance of OA across the entire domain, Task 5 assessed the extent of oxidation (using various metrics) of organic PM across Houston. In general, upwind locations (in the southeast of Houston) exhibit OA that is relatively more oxidized, indicating regional influence (aged SOA) on the sampled OA. Sampling in the center of Houston shows more reduced OA (on a relative scale) due to the influence of primary emissions from motor vehicles and industrial point sources. Downwind locations are characterized by OA that is medium on the oxidation scale due to the combination of local influences, primary emissions, and photochemical aging.

The information garnered by Task 5 also is relevant for Task 6, which evaluated the importance of secondary processes in the formation of PM in Houston, including SOA described by the oxidation metrics referenced above. Here, PMF was used to apportion OA to multiple factors that can be linked to sources. Based on PMF output, sulfate and more aged SOA (OOA-II) appear to be influenced by regional rather than local activities. Ammonium concentrations track those of sulfate, but the extent of neutralization with regard to gas-phase ammonia could not be evaluated due to the limited amount of data. The local formation of SOA (OOA-I) appears to be influenced significantly by monoterpene-nitrate radical chemistry, particularly in the northwest. Relationships between LWC and SOA are temporally and spatially variable, and it appears that LWC (as an absorptive medium) is not necessary for OOA formation.

Task 7 attempted to combine gas- and particle-phase data by investigating the importance of BVOCs in O_3 and SOA formation in Houston. As found in Task 6, monoterpene reactions with nitrate radical appear to influence SOA formation; however,

isoprene appears to have less significant importance with regard specifically to SOA. In contrast, O_3 formation appears to be very sensitive to isoprene based on photochemical box modeling performed for Manvel Croix and Conroe sampling sites.

Task 8 considered a comparison of *in situ* (ground-based monitors) and column (ground-based Pandora, airplane, and satellite) measurements of NO_2. The comparison of *in situ* with column measurements is impacted extensively by the spatial and temporal resolution of the measurements as well as assumptions about mixing within the planetary boundary layer.

Finally, Tasks 9 and 10 allowed quantification of O_3 production/destruction rates and radical source strengths across Houston using the LARC photochemical box model. The rates of O_3 production and destruction are most realistic in the two locations of interest (Conroe and Manvel Croix) when the P-3B-all case is used for VOC mixing ratios. In this case, airplane spiral data is used to correct VOC mixing ratios estimated based on pollution level, wind direction, and CMAQ. The diurnal profiles of these processes are realistic given known meteorology. The formation of O_3 consistently is governed by HO_2 plus NO reactions (approximately half), RO_2 plus NO reactions (slightly more than one third), and CH_3O_2 plus NO reactions (the remainder). Aldehyde and isoprene chemistries play significant roles in RO_2 formation. The loss of O_3 is primarily caused by HNO_3 formation.

Future Work, Recommendations, and Concluding Remarks

To further characterize differences in derived EF measured on-road, a targeted motor vehicle emissions study was performed using the MAQL during spring 2015. Rather than relying on chance encounters with vehicles, as with much of the DISCOVER-AQ study, this new study deployed the MAQL at specific sites to measure vehicular emissions. The novel method presented here will be used for the new data, with the results determining the best method by which to estimate motor vehicle EF values for OA. However, analysis and characterization of the more recent data falls outside of the current project, which focuses solely on DISCOVER-AQ. Therefore, no further information is provided here.

The PARAFAC analysis will be conducted based on the application of two different mathematical algorithms: PMF3 and Multilinear Engine 2. The application of PARAFAC to the high-resolution dataset generated during DISCOVER-AQ likely will allow the identification of additional aerosol components and will provide more robust information of the size distribution of these. However, it should be noted that PMF output is required as PARAFAC input and that PARAFAC was not included in the original project work description. It is currently under investigation.

It is also important to consider additional future field measurements in Houston using the MAQL (or multiple mobile facilities). This would allow characterization of the spatial and temporal profiles of air quality (most specifically PM) in Houston to a much more significant extent, which is especially important given the spatial and temporal patterns observed here. Specifically, a Lagrangian study would be ideal to study in-plume transformations. Modeling of OH sources and sinks also would be of interest.

The results described here are currently being converted into manuscripts for publication. It is predicted that six manuscripts related to this project will be published.

Based on this work, several recommendations can be made to help improve air quality with respect to PM in Houston. Based on the large emission rates observed for motor vehicles, it is imperative that efforts to limit emissions from these sources continue, including vehicle monitoring programs and traffic control systems. Regulation of industrial facilities also must continue, and local ordinances with respect to open burning of biomass are recommended. Given the apparent influence of nitrate radical chemistry on OOA-I formation, future work should investigate how NO controls alter potential SOA formation in the Houston environment. The impact is hypothesized to be highly non-linear given that NO impacts O_3, which further impacts the formation of OH, which then influences SOA through oxidation of both anthropogenic and biogenic VOC precursors. Additional modeling studies should investigate how Houston's high humidity impacts local SOA formation so that such information can be integrated into control strategies. It is known that humidity is not controllable, but the species that lead to significant aerosol LWC (predominantly sulfate, nitrate, and ammonium) because of their interaction with water vapor are. In conclusion, this project has noted the large variability in PM across Houston in terms of concentrations, extent of oxidation, and probable sources. As Houston continues to remain barely in compliance with PM NAAQS, this study emphasizes the importance of continued PM studies.

References

Aiken, A.C. et al., 2008. O/C and OM/OC ratios of primary, secondary, and ambient organic aerosols with high-resolution time-of-flight aerosol mass spectrometry. *Environ. Sci. Technol. 42*, 4478-4485.

Canagaratna, M. et al., 2007. Chemical and microphysical characterization of ambient aerosols with the Aerodyne aerosol mass spectrometer. *Mass Spec. Rev. 26*, 185-222.

Canagaratna, M. et al., 2015. Elemental ratio measurements of organic compounds using aerosol mass spectrometry: Characterization, improved calibration, and implications. *Atmos. Chem. Phys. 15*, 253-272.

Cleveland, M.J. et al., 2012. Characterization of urban aerosol using aerosol mass spectrometry and proton nuclear magnetic resonance spectroscopy. *Atmos. Environ. 54*, 511-518.

Czader, B.H. et al., 2015. Impact of updated traffic emissions on HONO mixing ratios simulated for urban site in Houston, Texas. *Atmos. Chem. Phys. 15*, 1253-1263.

Kroll, J.H. et al., 2011. Carbon oxidation state as a metric for describing the chemistry of atmospheric organic aerosol. *Nature Chem. 3*, 133-139.

Nenes, A. et al., 1998. ISORROPIA: A new thermodynamic equilibrium model for multiphase multicomponent inorganic aerosols. *Aquat. Geochem. 4*, 123-152.

Olson, J.R. et al., 2006. A reevaluation of airborne HO_x observations from NASA field campaigns. *J. Geophys. Res. – Atmos. 111*, doi:10.1029/2005JD006617.

Stutz, J. et al., 2010. Nocturnal NO_3 radical chemistry in Houston, TX. *Atmos. Environ. 44*, 4099-4106.

Ulbrich, I. et al., 2009. Interpretation of organic components from Positive Matrix Factorization of aerosol mass spectrometric data. *Atmos. Chem. Phys. 9*, 2891-2918.

Wexler, A.S., and S.L. Clegg, 2002. Atmospheric aerosol models for systems including the ions H^+, NH_4^+, Na^+, SO_4^{2-}, NO_3^-, Cl^-, Br^-, and H_2O. *J. Geophys. Res. – Atmos. 107*, doi:10.1029/2001JD000451.

Wojcik, G.S., and J.S. Chang, 1997. A reevaluation of sulfur budgets, lifetimes, and scavenging ratios for eastern North America. *J. Atmos. Chem. 26*, 109-145.